

# Flow of Non-Newtonian Fluids in Porous Media

Taha Sochi\*

2010

---

\*University College London, Department of Physics & Astronomy, Gower Street, London, WC1E 6BT. Email: t.sochi@ucl.ac.uk.

# Contents

<b>Contents</b>	<b>ii</b>
<b>List of Figures</b>	<b>iv</b>
<b>List of Tables</b>	<b>iv</b>
<b>Abstract</b>	<b>1</b>
<b>1 Introduction</b>	<b>2</b>
1.1 Time-Independent Fluids . . . . .	7
1.1.1 Power-Law Model . . . . .	8
1.1.2 Ellis Model . . . . .	8
1.1.3 Carreau Model . . . . .	9
1.1.4 Herschel-Bulkley Model . . . . .	10
1.2 Viscoelastic Fluids . . . . .	11
1.2.1 Maxwell Model . . . . .	13
1.2.2 Jeffreys Model . . . . .	14
1.2.3 Upper Convected Maxwell (UCM) Model . . . . .	14
1.2.4 Oldroyd-B Model . . . . .	15
1.2.5 Bautista-Manero Model . . . . .	16
1.3 Time-Dependent Fluids . . . . .	17
1.3.1 Godfrey Model . . . . .	18
1.3.2 Stretched Exponential Model . . . . .	18
<b>2 Modeling the Flow of Fluids</b>	<b>19</b>
2.1 Modeling Flow in Porous Media . . . . .	20
2.1.1 Continuum Models . . . . .	20
2.1.2 Capillary Bundle Models . . . . .	24
2.1.3 Numerical Methods . . . . .	27
2.1.4 Pore-Scale Network Modeling . . . . .	28
<b>3 Yield-Stress</b>	<b>37</b>
3.1 Modeling Yield-Stress in Porous Media . . . . .	38
3.2 Predicting Threshold Yield Pressure (TYP) . . . . .	40
3.2.1 Minimum Threshold Path Approach . . . . .	40
3.2.2 Percolation Theory Approach . . . . .	43

<b>4</b>	<b>Viscoelasticity</b>	<b>45</b>
4.1	Important Aspects for Flow in Porous Media . . . . .	47
4.1.1	Extensional Flow . . . . .	48
4.1.2	Converging-Diverging Geometry . . . . .	52
4.2	Viscoelastic Effects in Porous Media . . . . .	53
4.2.1	Transient Time-Dependence . . . . .	55
4.2.2	Steady-State Time-Dependence . . . . .	55
4.2.3	Dilatancy at High Flow Rates . . . . .	57
<b>5</b>	<b>Thixotropy and Rheopexy</b>	<b>60</b>
5.1	Modeling Time-Dependent Flow in Porous Media . . . . .	63
<b>6</b>	<b>Experimental Work</b>	<b>65</b>
<b>7</b>	<b>Conclusions</b>	<b>69</b>
<b>8</b>	<b>Terminology of Flow and Viscoelasticity</b>	<b>70</b>
<b>9</b>	<b>Nomenclature</b>	<b>75</b>
	<b>References</b>	<b>78</b>
	<b>Index</b>	<b>94</b>

## List of Figures

1	The six main classes of the time-independent fluids presented in a generic graph of stress against strain rate in shear flow . . . . .	5
2	Typical time-dependence behavior of viscoelastic fluids due to delayed response and relaxation following a step increase in strain rate	5
3	Intermediate plateau typical of <i>in situ</i> viscoelastic behavior due to time characteristics of the fluid and flow system and converging-diverging nature of the flow channels . . . . .	6
4	Strain hardening at high strain rates typical of <i>in situ</i> viscoelastic flow attributed to the dominance of extension over shear at high flow rates . . . . .	6
5	The two classes of time-dependent fluids compared to the time-independent presented in a generic graph of stress against time . . .	7
6	The bulk rheology of a power-law fluid on logarithmic scales for finite shear rates ( $\dot{\gamma} > 0$ ) . . . . .	8
7	The bulk rheology of an Ellis fluid on logarithmic scales for finite shear rates ( $\dot{\gamma} > 0$ ) . . . . .	9
8	The bulk rheology of a Carreau fluid on logarithmic scales for finite shear rates ( $\dot{\gamma} > 0$ ) . . . . .	10
9	Examples of corrugated capillaries that can be used to model converging-diverging geometry in porous media . . . . .	34
10	Typical behavior of shear viscosity $\mu_s$ as a function of shear rate $\dot{\gamma}$ in shear flow on log-log scales . . . . .	51
11	Typical behavior of extensional viscosity $\mu_x$ as a function of extension rate $\dot{\epsilon}$ in extensional flow on log-log scales . . . . .	51
12	Comparison between time dependency in thixotropic and viscoelastic fluids following a step increase in strain rate . . . . .	62

## List of Tables

1	Commonly used forms of the three popular continuum models . . .	21
---	---	----

## **Abstract**

The study of flow of non-Newtonian fluids in porous media is very important and serves a wide variety of practical applications in processes such as enhanced oil recovery from underground reservoirs, filtration of polymer solutions and soil remediation through the removal of liquid pollutants. These fluids occur in diverse natural and synthetic forms and can be regarded as the rule rather than the exception. They show very complex strain and time dependent behavior and may have initial yield-stress. Their common feature is that they do not obey the simple Newtonian relation of proportionality between stress and rate of deformation. Non-Newtonian fluids are generally classified into three main categories: time-independent whose strain rate solely depends on the instantaneous stress, time-dependent whose strain rate is a function of both magnitude and duration of the applied stress and viscoelastic which shows partial elastic recovery on removal of the deforming stress and usually demonstrates both time and strain dependency. In this article the key aspects of these fluids are reviewed with particular emphasis on single-phase flow through porous media. The four main approaches for describing the flow in porous media are examined and assessed. These are: continuum models, bundle of tubes models, numerical methods and pore-scale network modeling.

## 1 Introduction

Newtonian fluids are defined to be those fluids exhibiting a direct proportionality between stress  $\tau$  and strain rate  $\dot{\gamma}$  in laminar flow, that is

$$\tau = \mu\dot{\gamma} \quad (1)$$

where the viscosity  $\mu$  is independent of the strain rate although it might be affected by other physical parameters, such as temperature and pressure, for a given fluid system. A stress versus strain rate graph for a Newtonian fluid will be a straight line through the origin [1, 2]. In more precise technical terms, Newtonian fluids are characterized by the assumption that the extra stress tensor, which is the part of the total stress tensor that represents the shear and extensional stresses caused by the flow excluding hydrostatic pressure, is a linear isotropic function of the components of the velocity gradient, and therefore exhibits a linear relationship between stress and the rate of strain [3–5]. In tensor form, which takes into account both shear and extension flow components, this linear relationship is expressed by

$$\boldsymbol{\tau} = \mu\dot{\boldsymbol{\gamma}} \quad (2)$$

where  $\boldsymbol{\tau}$  is the extra stress tensor and  $\dot{\boldsymbol{\gamma}}$  is the rate of strain tensor which describes the rate at which neighboring particles move with respect to each other independent of superposed rigid rotations. Newtonian fluids are generally featured by having shear- and time-independent viscosity, zero normal stress differences in simple shear flow, and simple proportionality between the viscosities in different types of deformation [6, 7].

All those fluids for which the proportionality between stress and strain rate is violated, due to nonlinearity or initial yield-stress, are said to be non-Newtonian. Some of the most characteristic features of non-Newtonian behavior are: strain-dependent viscosity as the viscosity depends on the type and rate of deformation, time-dependent viscosity as the viscosity depends on duration of deformation, yield-stress where a certain amount of stress should be reached before the flow starts, and stress relaxation where the resistance force on stretching a fluid element will first rise sharply then decay with a characteristic relaxation time.

Non-Newtonian fluids are commonly divided into three broad groups, although in reality these classifications are often by no means distinct or sharply defined

[1, 2]:

1. Time-independent fluids are those for which the strain rate at a given point is solely dependent upon the instantaneous stress at that point.
2. Viscoelastic fluids are those that show partial elastic recovery upon the removal of a deforming stress. Such materials possess properties of both viscous fluids and elastic solids.
3. Time-dependent fluids are those for which the strain rate is a function of both the magnitude and the duration of stress and possibly of the time lapse between consecutive applications of stress.

Those fluids that exhibit a combination of properties from more than one of the above groups are described as complex fluids [8], though this term may be used for non-Newtonian fluids in general.

The generic rheological behavior of the three groups of non-Newtonian fluids is graphically presented in Figures (1-5). Figure (1) demonstrates the six principal rheological classes of the time-independent fluids in shear flow. These represent shear-thinning, shear-thickening and shear-independent fluids each with and without yield-stress. It is worth noting that these rheological classes are idealizations as the rheology of these fluids is generally more complex and they can behave differently under various deformation and ambient conditions. However, these basic rheological trends can describe the behavior under particular circumstances and the overall behavior consists of a combination of stages each modeled with one of these basic classes.

Figures (2-4) display several aspects of the rheology of viscoelastic fluids in bulk and *in situ*. In Figure (2) a stress versus time graph reveals a distinctive feature of time-dependency largely observed in viscoelastic fluids. As seen, the overshoot observed on applying a sudden deformation cycle relaxes eventually to the equilibrium steady-state. This time-dependent behavior has an impact not only on the flow development in time, but also on the dilatancy behavior observed in porous media flow under steady-state conditions. The converging-diverging geometry contributes to the observed increase in viscosity when the relaxation time characterizing the fluid becomes comparable in size to the characteristic time of the flow, as will be discussed in Section (4).

Figure (3) reveals another characteristic feature of viscoelasticity observed in porous media flow. The intermediate plateau may be attributed to the time-dependent nature of the viscoelastic fluid when the relaxation time of the fluid and the characteristic time of the flow become comparable in size. This behavior may also be attributed to build-up and break-down due to sudden change in radius and hence rate of strain on passing through the converging-diverging pores. A thixotropic nature will be more appropriate in this case.

Figure (4) presents another typical feature of viscoelastic fluids. In addition to the low-deformation Newtonian plateau and the shear-thinning region which are widely observed in many time-independent fluids and modeled by various time-independent rheological models, there is a thickening region which is believed to be originating from the dominance of extension over shear at high flow rates. This feature is mainly observed in the flow through porous media, and the converging-diverging geometry is usually given as an explanation for the shift in dominance from shear to extension at high flow rates.

In Figure (5) the two basic classes of time-dependent fluids are presented and compared to the time-independent fluid in a graph of stress versus time of deformation under constant strain rate condition. As seen, thixotropy is the equivalent in time to shear-thinning, while rheopexy is the equivalent in time to shear-thickening.

A large number of models have been proposed in the literature to model all types of non-Newtonian fluids under diverse flow conditions. However, the majority of these models are basically empirical in nature and arise from curve-fitting exercises [7]. In the following sections, the three groups of non-Newtonian fluids will be investigated and a few prominent examples of each group will be presented.

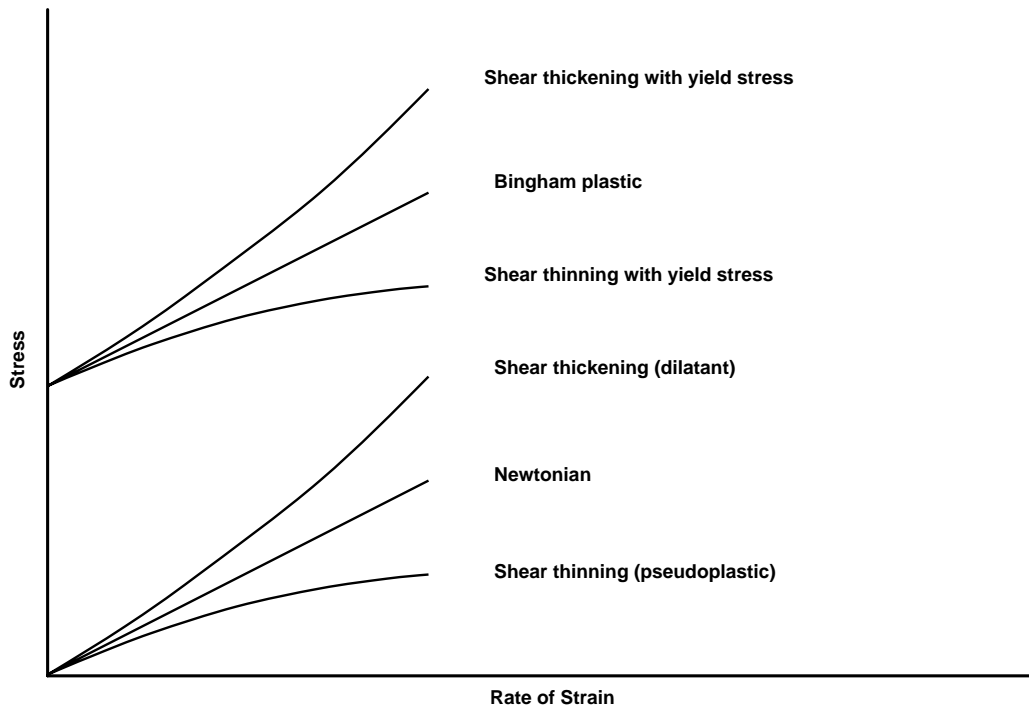


Figure 1: The six main classes of the time-independent fluids presented in a generic graph of stress against strain rate in shear flow.

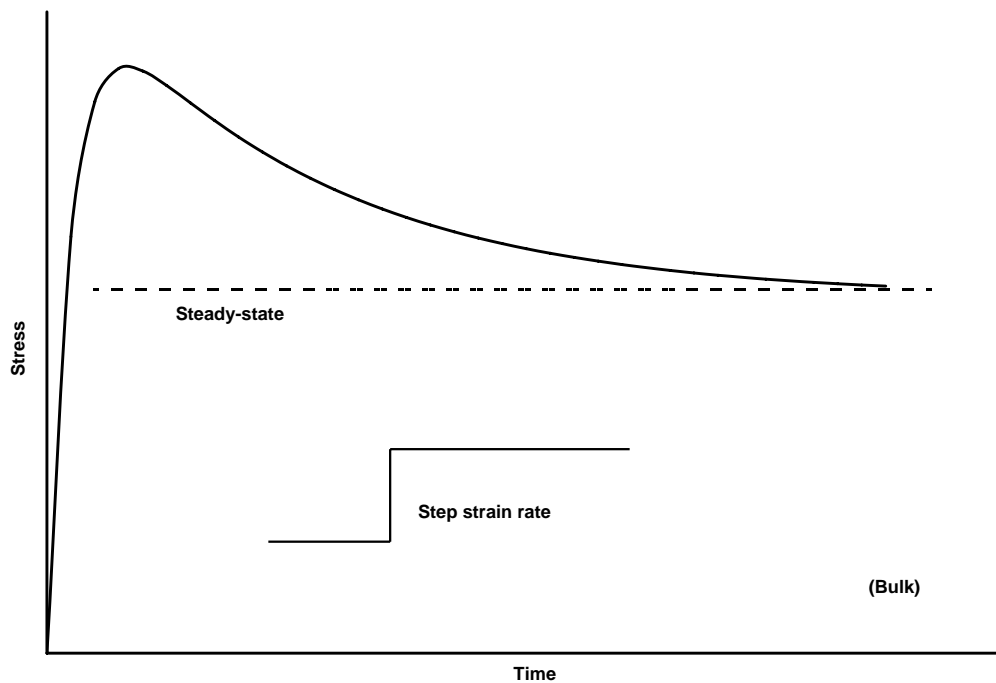


Figure 2: Typical time-dependence behavior of viscoelastic fluids due to delayed response and relaxation following a step increase in strain rate.

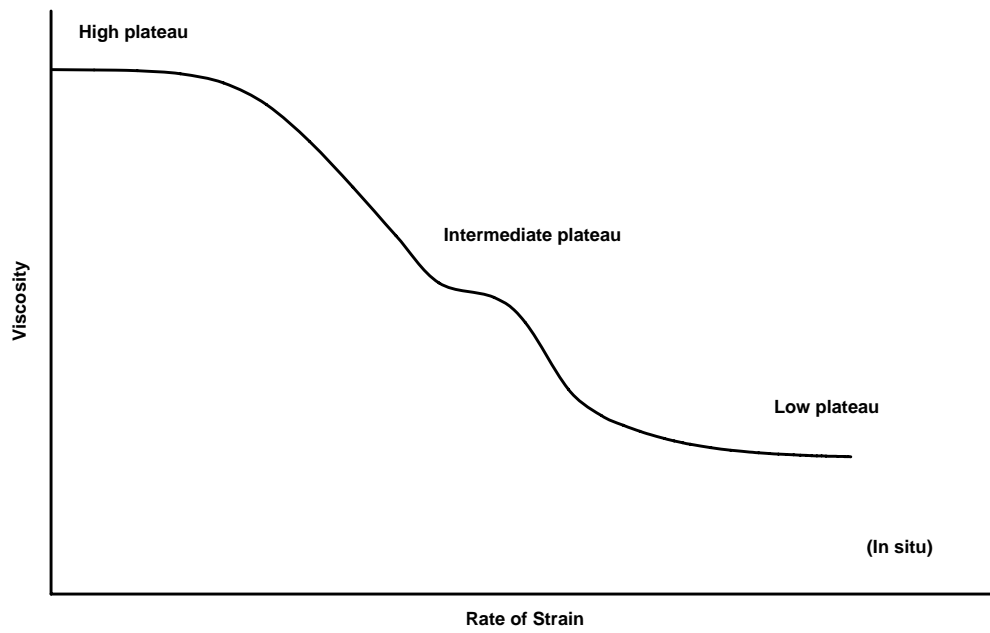


Figure 3: Intermediate plateau typical of *in situ* viscoelastic behavior due to time characteristics of the fluid and flow system and converging-diverging nature of the flow channels.

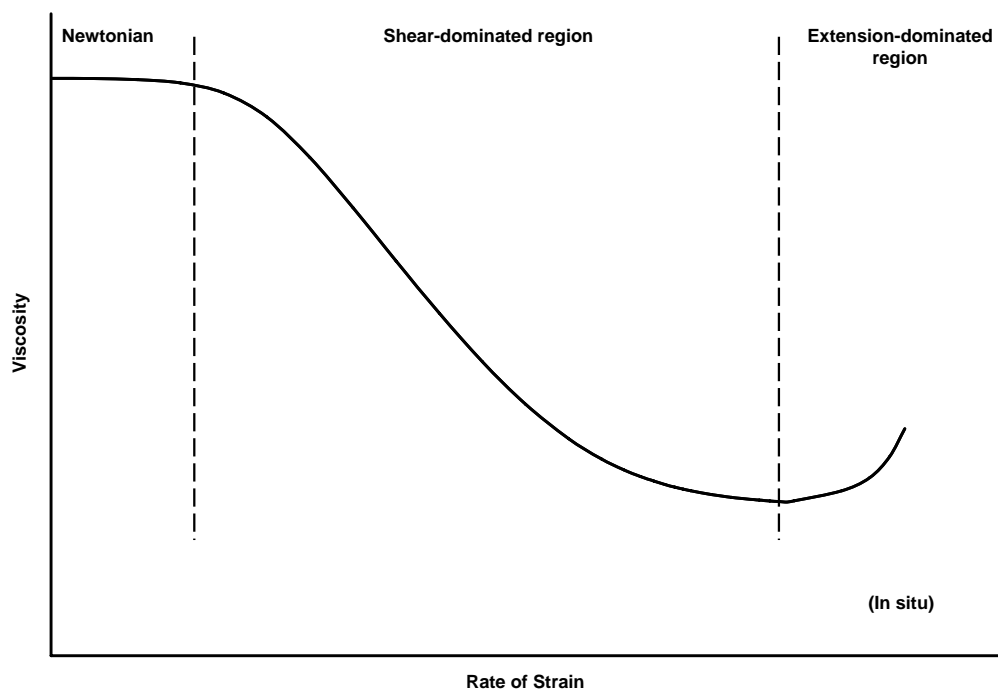


Figure 4: Strain hardening at high strain rates typical of *in situ* viscoelastic flow attributed to the dominance of extension over shear at high flow rates.

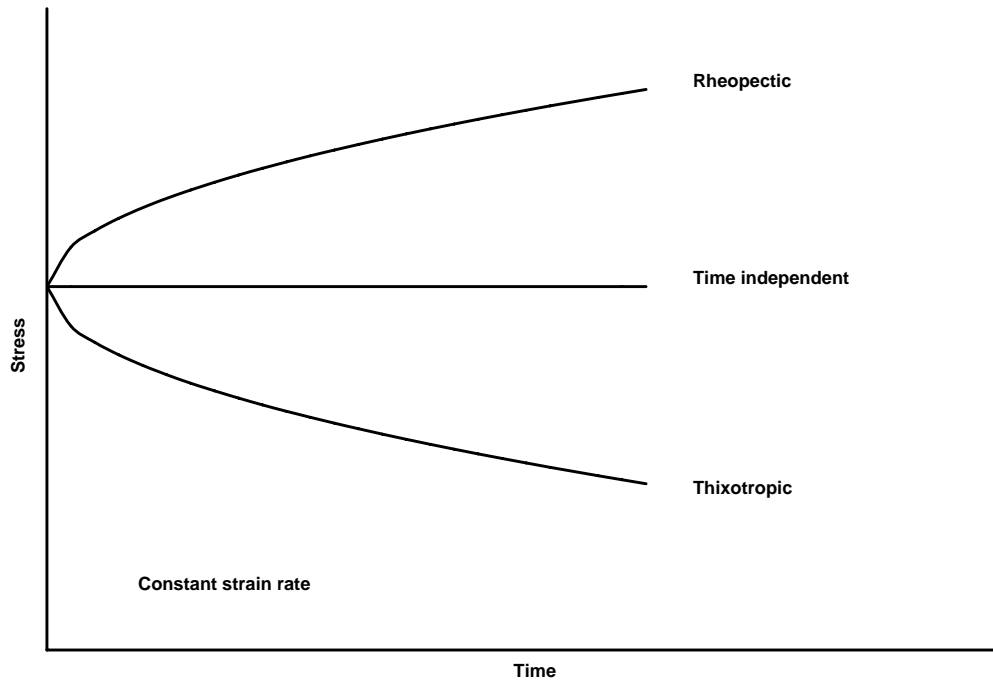


Figure 5: The two classes of time-dependent fluids compared to the time-independent presented in a generic graph of stress against time.

## 1.1 Time-Independent Fluids

Shear rate dependence is one of the most important and defining characteristics of non-Newtonian fluids in general and time-independent fluids in particular. When a typical non-Newtonian fluid experiences a shear flow the viscosity appears to be Newtonian at low shear rates. After this initial Newtonian plateau the viscosity is found to vary with increasing shear rate. The fluid is described as shear-thinning or pseudoplastic if the viscosity decreases, and shear-thickening or dilatant if the viscosity increases on increasing shear rate. After this shear-dependent regime, the viscosity reaches a limiting constant value at high shear rate. This region is described as the upper Newtonian plateau. If the fluid sustains initial stress without flowing, it is called a yield-stress fluid. Almost all polymer solutions that exhibit a shear rate dependent viscosity are shear-thinning, with relatively few polymer solutions demonstrating dilatant behavior. Moreover, in most known cases of shear-thickening there is a region of shear-thinning at lower shear rates [3, 6, 7].

In this article, we present four fluid models of the time-independent group: power-law, Ellis, Carreau and Herschel-Bulkley. These are widely used in modeling non-Newtonian fluids of this group.

### 1.1.1 Power-Law Model

The power-law, or Ostwald-de Waele model, is one of the simplest time-independent fluid models as it contains only two parameters. The model is given by the relation [6, 9]

$$\mu = C\dot{\gamma}^{n-1} \quad (3)$$

where  $\mu$  is the viscosity,  $C$  is the consistency factor,  $\dot{\gamma}$  is the shear rate and  $n$  is the flow behavior index. In Figure (6), the bulk rheology of this model for shear-thinning case is presented in a generic form as viscosity versus shear rate on log-log scales. The power-law is usually used to model shear-thinning though it can also be used for modeling shear-thickening by making  $n > 1$ . The major weakness of power-law model is the absence of plateaux at low and high shear rates. Consequently, it fails to produce sensible results in these shear regimes.

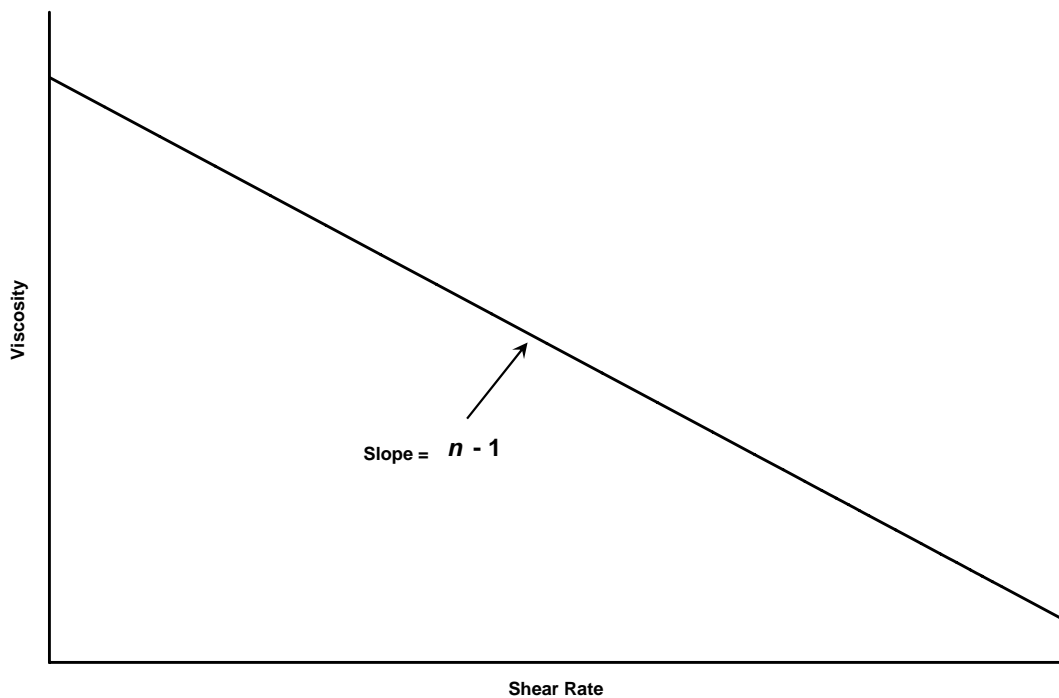


Figure 6: The bulk rheology of a power-law fluid on logarithmic scales for finite shear rates ( $\dot{\gamma} > 0$ ).

### 1.1.2 Ellis Model

This is a three-parameter model that describes time-independent shear-thinning non-yield-stress fluids. It is used as a substitute for the power-law model and is

appreciably better than the power-law in matching experimental measurements. Its distinctive feature is the low-shear Newtonian plateau without a high-shear plateau. According to this model, the fluid viscosity  $\mu$  is given by [6, 9–12]

$$\mu = \frac{\mu_o}{1 + \left(\frac{\tau}{\tau_{1/2}}\right)^{\alpha-1}} \quad (4)$$

where  $\mu_o$  is the low-shear viscosity,  $\tau$  is the shear stress,  $\tau_{1/2}$  is the shear stress at which  $\mu = \mu_o/2$  and  $\alpha$  is an indicial parameter related to the power-law index by  $\alpha = 1/n$ . A generic graph demonstrating the bulk rheology, that is viscosity versus shear rate on logarithmic scales, is shown in Figure (7).

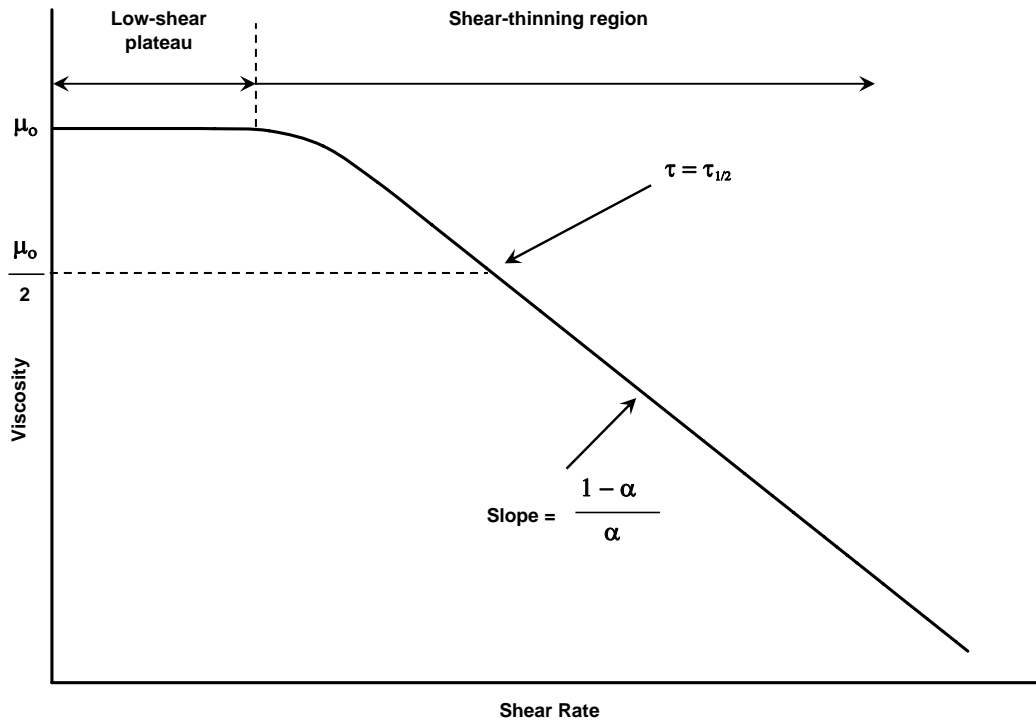


Figure 7: The bulk rheology of an Ellis fluid on logarithmic scales for finite shear rates ( $\dot{\gamma} > 0$ ).

### 1.1.3 Carreau Model

This is a four-parameter rheological model that can describe shear-thinning fluids with no yield-stress. It is generally praised for its compliance with experiment. The distinctive feature of this model is the presence of low- and high-shear plateaux.

The Carreau fluid is given by the relation [9]

$$\mu = \mu_{\infty} + \frac{\mu_o - \mu_{\infty}}{[1 + (\dot{\gamma}t_c)^2]^{\frac{1-n}{2}}} \quad (5)$$

where  $\mu$  is the fluid viscosity,  $\mu_{\infty}$  is the viscosity at infinite shear rate,  $\mu_o$  is the viscosity at zero shear rate,  $\dot{\gamma}$  is the shear rate,  $t_c$  is a characteristic time and  $n$  is the flow behavior index. A generic graph demonstrating the bulk rheology is shown in Figure (8).

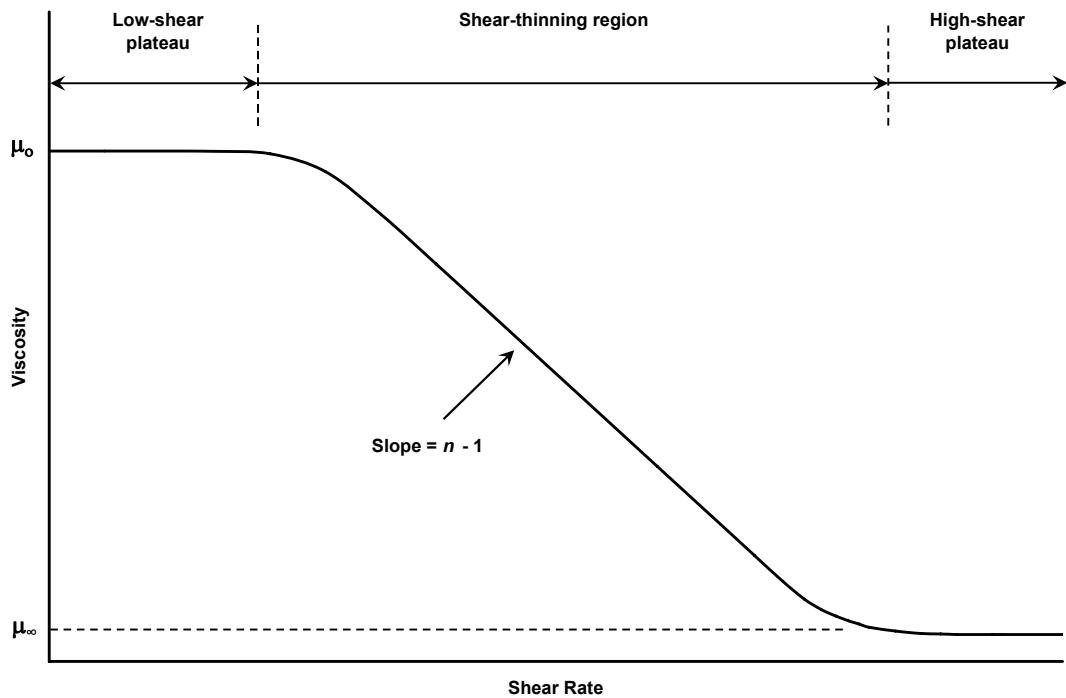


Figure 8: The bulk rheology of a Carreau fluid on logarithmic scales for finite shear rates ( $\dot{\gamma} > 0$ ).

#### 1.1.4 Herschel-Bulkley Model

The Herschel-Bulkley is a simple rheological model with three parameters. Despite its simplicity it can describe the Newtonian and all main classes of the time-independent non-Newtonian fluids. It is given by the relation [1, 9, 12]

$$\tau = \tau_o + C\dot{\gamma}^n \quad (\tau > \tau_o) \quad (6)$$

where  $\tau$  is the shear stress,  $\tau_o$  is the yield-stress above which the substance starts to flow,  $C$  is the consistency factor,  $\dot{\gamma}$  is the shear rate and  $n$  is the flow behavior

index. The Herschel-Bulkley model reduces to the power-law when  $\tau_o = 0$ , to the Bingham plastic when  $n = 1$ , and to the Newton's law for viscous fluids when both these conditions are satisfied.

There are six main classes to this model:

- |                                       |                       |
|---------------------------------------|-----------------------|
| 1. Shear-thinning (pseudoplastic)     | $[\tau_o = 0, n < 1]$ |
| 2. Newtonian                          | $[\tau_o = 0, n = 1]$ |
| 3. Shear-thickening (dilatant)        | $[\tau_o = 0, n > 1]$ |
| 4. Shear-thinning with yield-stress   | $[\tau_o > 0, n < 1]$ |
| 5. Bingham plastic                    | $[\tau_o > 0, n = 1]$ |
| 6. Shear-thickening with yield-stress | $[\tau_o > 0, n > 1]$ |

These classes are graphically illustrated in Figure (1).

## 1.2 Viscoelastic Fluids

Polymeric fluids often show strong viscoelastic effects. These include shear-thinning, extension-thickening, normal stresses, and time-dependent rheology. No theory is yet available that can adequately describe all of the observed viscoelastic phenomena in a variety of flows. Nonetheless, many differential and integral constitutive models have been proposed in the literature to describe viscoelastic flow. What is common to all these is the presence of at least one characteristic time parameter to account for the fluid memory, that is the stress at the present time depends upon the strain or rate of strain for all past times, but with a fading memory [3, 13–16].

Broadly speaking, viscoelasticity is divided into two major fields: linear and nonlinear. **Linear viscoelasticity** is the field of rheology devoted to the study of viscoelastic materials under very small strain or deformation where the displacement gradients are very small and the flow regime can be described by a linear relationship between stress and rate of strain. In principle, the strain has to be sufficiently small so that the structure of the material remains unperturbed by the flow history. If the strain rate is small enough, deviation from linear viscoelasticity may not occur at all. The equations of linear viscoelasticity are not valid for

deformations of arbitrary magnitude and rate because they violate the principle of frame invariance. The validity of linear viscoelasticity when the small-deformation condition is satisfied with a large magnitude of rate of strain is still an open question, though it is widely accepted that linear viscoelastic constitutive equations are valid in general for any strain rate as long as the total strain remains small. Nevertheless, the higher the strain rate the shorter the time at which the critical strain for departure from linear regime is reached [6, 9, 17].

The linear viscoelastic models have several limitations. For example, they cannot describe strain rate dependence of viscosity or normal stress phenomena since these are nonlinear effects. Due to the restriction to infinitesimal deformations, the linear models may be more appropriate for the description of viscoelastic solids rather than viscoelastic fluids. Despite the limitations of the linear viscoelastic models and despite being of less interest to the study of flow where the material is usually subject to large deformation, they are very important in the study of viscoelasticity for several reasons [6, 9, 18]:

1. They are used to characterize the behavior of viscoelastic materials at small deformations.
2. They serve as a motivation and starting point for developing nonlinear models since the latter are generally extensions to the linears.
3. They are used for analyzing experimental data obtained in small deformation experiments and for interpreting important viscoelastic phenomena, at least qualitatively.

**Non-linear viscoelasticity** is the field of rheology devoted to the study of viscoelastic materials under large deformation, and hence it is the subject of primary interest to the study of flow of viscoelastic fluids. Nonlinear viscoelastic constitutive equations are sufficiently complex that very few flow problems can be solved analytically. Moreover, there appears to be no differential or integral constitutive equation general enough to explain the observed behavior of polymeric systems undergoing large deformations but still simple enough to provide a basis for engineering design procedures [1, 6, 19].

As the linear viscoelasticity models are not valid for deformations of large magnitude because they do not satisfy the principle of frame invariance, Oldroyd and

others tried to extend these models to nonlinear regimes by developing a set of frame-invariant constitutive equations. These equations define time derivatives in frames that deform with the material elements. Examples include rotational, upper and lower convected time derivatives. The idea of these derivatives is to express the constitutive equation in real space coordinates rather than local coordinates and hence fulfilling the Oldroyd's admissibility criteria for constitutive equations. These admissibility criteria ensures that the equations are invariant under a change of coordinate system, value invariant under a change of translational or rotational motion of the fluid element as it goes through space, and value invariant under a change of rheological history of neighboring fluid elements [6, 18].

There is a large number of rheological equations proposed for the description of nonlinear viscoelasticity, as a quick survey to the literature reveals. However, many of these models are extensions or modifications to others. The two most popular nonlinear viscoelastic models in differential form are the Upper Convected Maxwell and the Oldroyd-B models.

In the following sections we present two linear and three nonlinear viscoelastic models in differential form.

### 1.2.1 Maxwell Model

This is the first known attempt to obtain a viscoelastic constitutive equation. This simple linear model, with only one elastic parameter, combines the ideas of viscosity of fluids and elasticity of solids to arrive at an equation for viscoelastic materials [6, 20]. Maxwell [21] proposed that fluids with both viscosity and elasticity can be described, in modern notation, by the relation:

$$\boldsymbol{\tau} + \lambda_1 \frac{\partial \boldsymbol{\tau}}{\partial t} = \mu_o \dot{\boldsymbol{\gamma}} \quad (7)$$

where  $\boldsymbol{\tau}$  is the extra stress tensor,  $\lambda_1$  is the fluid relaxation time,  $t$  is time,  $\mu_o$  is the low-shear viscosity and  $\dot{\boldsymbol{\gamma}}$  is the rate of strain tensor.

### 1.2.2 Jeffreys Model

This is a linear model proposed as an extension to the Maxwell model by including a time derivative of the strain rate, that is [6, 22]:

$$\boldsymbol{\tau} + \lambda_1 \frac{\partial \boldsymbol{\tau}}{\partial t} = \mu_o \left( \dot{\boldsymbol{\gamma}} + \lambda_2 \frac{\partial \dot{\boldsymbol{\gamma}}}{\partial t} \right) \quad (8)$$

where  $\lambda_2$  is the retardation time that accounts for the corrections of this model and can be seen as a measure of the time the material needs to respond to deformation. The Jeffreys model has three constants: a viscous parameter  $\mu_o$ , and two elastic parameters,  $\lambda_1$  and  $\lambda_2$ . The model reduces to the linear Maxwell when  $\lambda_2 = 0$ , and to the Newtonian when  $\lambda_1 = \lambda_2 = 0$ . As observed by several authors, the Jeffreys model is one of the most suitable linear models to compare with experiment [23].

### 1.2.3 Upper Convected Maxwell (UCM) Model

To extend the linear Maxwell model to the nonlinear regime, several time derivatives (e.g. upper convected, lower convected and corotational) have been proposed to replace the ordinary time derivative in the original model. The most commonly used of these derivatives in conjunction with the Maxwell model is the upper convected. On purely continuum mechanical grounds there is no reason to prefer one of these Maxwell equations to the others as they all satisfy frame invariance. The popularity of the upper convected form is due to its more realistic features [3, 9, 18].

The Upper Convected Maxwell (UCM) is the simplest nonlinear viscoelastic model and is one of the most popular models in numerical modeling and simulation of viscoelastic flow. Like its linear counterpart, it is a simple combination of the Newton's law for viscous fluids and the derivative of the Hook's law for elastic solids. Because of its simplicity, it does not fit the rich variety of viscoelastic effects that can be observed in complex rheological materials [23]. However, it is largely used as the basis for other more sophisticated viscoelastic models. It represents, like the linear Maxwell, purely elastic fluids with shear-independent viscosity, i.e. Boger fluids [24]. UCM also predicts an elongation viscosity that is three times the shear viscosity, like Newtonian, which is unrealistic feature for most viscoelastic fluids. The UCM model is obtained by replacing the partial time derivative in the differential form of the linear Maxwell with the upper convected time derivative,

that is

$$\boldsymbol{\tau} + \lambda_1 \overset{\nabla}{\boldsymbol{\tau}} = \mu_o \dot{\boldsymbol{\gamma}} \quad (9)$$

where  $\boldsymbol{\tau}$  is the extra stress tensor,  $\lambda_1$  is the relaxation time,  $\mu_o$  is the low-shear viscosity,  $\dot{\boldsymbol{\gamma}}$  is the rate of strain tensor, and  $\overset{\nabla}{\boldsymbol{\tau}}$  is the upper convected time derivative of the stress tensor. This time derivative is given by

$$\overset{\nabla}{\boldsymbol{\tau}} = \frac{\partial \boldsymbol{\tau}}{\partial t} + \mathbf{v} \cdot \nabla \boldsymbol{\tau} - (\nabla \mathbf{v})^T \cdot \boldsymbol{\tau} - \boldsymbol{\tau} \cdot \nabla \mathbf{v} \quad (10)$$

where  $t$  is time,  $\mathbf{v}$  is the fluid velocity,  $(\cdot)^T$  is the transpose of tensor and  $\nabla \mathbf{v}$  is the fluid velocity gradient tensor defined by Equation (29) in Appendix 8. The convected derivative expresses the rate of change as a fluid element moves and deforms. The first two terms in Equation (10) comprise the material or substantial derivative of the extra stress tensor. This is the time derivative following a material element and describes time changes taking place at a particular element of the ‘material’ or ‘substance’. The two other terms in (10) are the deformation terms. The presence of these terms, which account for convection, rotation and stretching of the fluid motion, ensures that the principle of frame invariance holds, that is the relationship between the stress tensor and the deformation history does not depend on the particular coordinate system used for the description. Despite the simplicity and limitations of the UCM model, it predicts important viscoelastic properties such as first normal stress difference in shear and strain hardening in elongation. It also predicts the existence of stress relaxation after cessation of flow and elastic recoil. However, according to the UCM the shear viscosity and the first normal stress difference are independent of shear rate and hence the model fails to describe the behavior of most viscoelastic fluids. Furthermore, it predicts a steady-state elongational viscosity that becomes infinite at a finite elongation rate, which is obviously far from physical reality [4, 6, 9, 18, 25, 26].

### 1.2.4 Oldroyd-B Model

The Oldroyd-B model is a simple form of the more elaborate and rarely used Oldroyd 8-constant model which also contains the upper convected, the lower convected, and the corotational Maxwell equations as special cases. Oldroyd-B is the second simplest nonlinear viscoelastic model and is apparently the most popular in viscoelastic flow modeling and simulation. It is the nonlinear equivalent of the linear Jeffreys model, as it takes account of frame invariance in the nonlinear regime.

Oldroyd-B model can be obtained by replacing the partial time derivatives in the differential form of the Jeffreys model with the upper convected time derivatives [6]

$$\boldsymbol{\tau} + \lambda_1 \overset{\nabla}{\boldsymbol{\tau}} = \mu_o \left( \dot{\boldsymbol{\gamma}} + \lambda_2 \overset{\nabla}{\dot{\boldsymbol{\gamma}}} \right) \quad (11)$$

where  $\overset{\nabla}{\dot{\boldsymbol{\gamma}}}$  is the upper convected time derivative of the rate of strain tensor given by

$$\overset{\nabla}{\dot{\boldsymbol{\gamma}}} = \frac{\partial \dot{\boldsymbol{\gamma}}}{\partial t} + \mathbf{v} \cdot \nabla \dot{\boldsymbol{\gamma}} - (\nabla \mathbf{v})^T \cdot \dot{\boldsymbol{\gamma}} - \dot{\boldsymbol{\gamma}} \cdot \nabla \mathbf{v} \quad (12)$$

Oldroyd-B model reduces to the UCM when  $\lambda_2 = 0$ , and to Newtonian when  $\lambda_1 = \lambda_2 = 0$ . Despite the simplicity of the Oldroyd-B model, it shows good qualitative agreement with experiments especially for dilute solutions of macromolecules and Boger fluids. The model is able to describe two of the main features of viscoelasticity, namely normal stress difference and stress relaxation. It predicts a constant viscosity and first normal stress difference with zero second normal stress difference. Moreover, the Oldroyd-B, like the UCM model, predicts an elongation viscosity that is three times the shear viscosity, as it is the case in Newtonian fluids. It also predicts an infinite extensional viscosity at a finite extensional rate, which is physically unrealistic [3, 6, 17, 23, 27].

A major limitation of the UCM and Oldroyd-B models is that they do not allow for strain dependency and second normal stress difference. To account for strain dependent viscosity and non-zero second normal stress difference among other phenomena, more sophisticated models such as Giesekus and Phan-Thien-Tanner (PTT) which introduce additional parameters should be considered. Such equations, however, have rarely been used because of the theoretical and experimental complications they introduce [28].

### 1.2.5 Bautista-Manero Model

This model combines the Oldroyd-B constitutive equation for viscoelasticity (11) and the Fredrickson's kinetic equation for flow-induced structural changes which may be associated with thixotropy. The model requires six parameters that have physical significance and can be estimated from rheological measurements. These parameters are the low and high shear rate viscosities, the elastic modulus, the relaxation time, and two other constants describing the build up and break down

of viscosity.

The kinetic equation of Fredrickson that accounts for the destruction and construction of structure is given by

$$\frac{d\mu}{dt} = \frac{\mu}{\lambda} \left(1 - \frac{\mu}{\mu_o}\right) + k\mu \left(1 - \frac{\mu}{\mu_\infty}\right) \boldsymbol{\tau} : \dot{\boldsymbol{\gamma}} \quad (13)$$

where  $\mu$  is the viscosity,  $t$  is the time of deformation,  $\lambda$  is the relaxation time upon the cessation of steady flow,  $\mu_o$  and  $\mu_\infty$  are the viscosities at zero and infinite shear rates respectively,  $k$  is a parameter that is related to a critical stress value below which the material exhibits primary creep,  $\boldsymbol{\tau}$  is the stress tensor and  $\dot{\boldsymbol{\gamma}}$  is the rate of strain tensor. In this model  $\lambda$  is a structural relaxation time whereas  $k$  is a kinetic constant for structure break down. The elastic modulus  $G_o$  is related to these parameters by  $G_o = \mu/\lambda$  [29–32].

The Bautista-Manero model was originally proposed for the rheology of worm-like micellar solutions which usually have an upper Newtonian plateau and show strong signs of shear-thinning. The model, which incorporates shear-thinning, elasticity and thixotropy, can be used to describe the complex rheological behavior of viscoelastic systems that also exhibit thixotropy and rheopexy under shear flow. It predicts stress relaxation, creep, and the presence of thixotropic loops when the sample is subjected to transient stress cycles. This model can also match steady shear, oscillatory and transient measurements of viscoelastic solutions [29–32].

### 1.3 Time-Dependent Fluids

It is generally recognized that there are two main types of time-dependent fluids: thixotropic (work softening) and rheopectic (work hardening or anti-thixotropic) depending upon whether the stress decreases or increases with time at a given strain rate and constant temperature. There is also a general consensus that the time-dependent feature is caused by reversible structural change during the flow process. However, there are many controversies about the details, and the theory of time-dependent fluids is not well developed. Many models have been proposed in the literature to describe the complex rheological behavior of time-dependent fluids. Here we present only two models of this group.

### 1.3.1 Godfrey Model

Godfrey [33] suggested that at a particular shear rate the time dependence of thixotropic fluids can be described by the relation

$$\mu(t) = \mu_i - \Delta\mu'(1 - e^{-t/\lambda'}) - \Delta\mu''(1 - e^{-t/\lambda''}) \quad (14)$$

where  $\mu(t)$  is the time-dependent viscosity,  $\mu_i$  is the viscosity at the commencement of deformation,  $\Delta\mu'$  and  $\Delta\mu''$  are the viscosity deficits associated with the decay time constants  $\lambda'$  and  $\lambda''$  respectively, and  $t$  is the time of shearing. The initial viscosity specifies a maximum value while the viscosity deficits specify the reduction associated with the particular time constants. As usual, the time constants define the time scales of the process under examination. Although Godfrey was originally proposed as a thixotropic model it can be easily extended to include rheopexy.

### 1.3.2 Stretched Exponential Model

This is a general time-dependent model that can describe both thixotropic and rheopectic rheologies [34]. It is given by

$$\mu(t) = \mu_i + (\mu_{inf} - \mu_i)(1 - e^{-(t/\lambda_s)^c}) \quad (15)$$

where  $\mu(t)$  is the time-dependent viscosity,  $\mu_i$  is the viscosity at the commencement of deformation,  $\mu_{inf}$  is the equilibrium viscosity at infinite time,  $t$  is the time of deformation,  $\lambda_s$  is a time constant and  $c$  is a dimensionless constant which in the simplest case is unity.

## 2 Modeling the Flow of Fluids

The basic equations describing the flow of fluids consist of the basic laws of continuum mechanics which are the conservation principles of mass, energy and linear and angular momentum. These governing equations indicate how the mass, energy and momentum of the fluid change with position and time. The basic equations have to be supplemented by a suitable rheological equation of state, or constitutive equation describing a particular fluid, which is a differential or integral mathematical relationship that relates the extra stress tensor to the rate of strain tensor in general flow condition and closes the set of governing equations. One then solves the constitutive model together with the conservation laws using a suitable method to predict the velocity and stress field of the flow. In the case of Navier-Stokes flows the constitutive equation is the Newtonian stress relation [4] as given in (2). In the case of more rheologically complex flows other non-Newtonian constitutive equations, such as Ellis and Oldroyd-B, should be used to bridge the gap and obtain the flow fields. To simplify the situation, several assumptions are usually made about the flow and the fluid. Common assumptions include laminar, incompressible, steady-state and isothermal flow. The last assumption, for instance, makes the energy conservation equation redundant [6, 9, 16, 35–39].

The constitutive equation should be frame-invariant. Consequently, sophisticated mathematical techniques are employed to satisfy this condition. No single choice of constitutive equation is best for all purposes. A constitutive equation should be chosen considering several factors such as the type of flow (shear or extension, steady or transient, etc.), the important phenomena to capture, the required level of accuracy, the available computational resources and so on. These considerations can be influenced strongly by personal preference or bias. Ideally the rheological equation of state is required to be as simple as possible, involving the minimum number of variables and parameters, and yet having the capability to predict the behavior of complex fluids in complex flows. So far, no constitutive equation has been developed that can adequately describe the behavior of complex fluids in general flow situation [3, 18]. Moreover, it is very unlikely that such an equation will be developed in the foreseeable future.

## 2.1 Modeling Flow in Porous Media

In the context of fluid flow, ‘porous medium’ can be defined as a solid matrix through which small interconnected cavities occupying a measurable fraction of its volume are distributed. These cavities are of two types: large ones, called pores and throats, which contribute to the bulk flow of fluid; and small ones, comparable to the size of the molecules, which do not have an impact on the bulk flow though they may participate in other transportation phenomena like diffusion. The complexities of the microscopic pore structure are usually avoided by resorting to macroscopic physical properties to describe and characterize the porous medium. The macroscopic properties are strongly related to the underlying microscopic structure. The best known examples of these properties are the porosity and the permeability. The first describes the relative fractional volume of the void space to the total volume while the second quantifies the capacity of the medium to transmit fluid. Another important property is the macroscopic homogeneity which may be defined as the absence of local variation in the relevant macroscopic properties, such as permeability, on a scale comparable to the size of the medium under consideration. Most natural and synthetic porous media have an element of inhomogeneity as the structure of the porous medium is typically very complex with a degree of randomness and can seldom be completely uniform. However, as long as the scale and magnitude of these variations have a negligible impact on the macroscopic properties under discussion, the medium can still be treated as homogeneous. The mathematical description of the flow in porous media is extremely complex and involves many approximations. So far, no analytical fluid mechanics solution to the flow through porous media has been developed. Furthermore, such a solution is apparently out of reach in the foreseeable future. Therefore, to investigate the flow through porous media other methodologies have been developed; the main ones are the continuum approach, the bundle of tubes approach, numerical methods and pore-scale network modeling. These approaches are outlined in the following sections with particular emphasis on the flow of non-Newtonian fluids [40–42].

### 2.1.1 Continuum Models

These widely used models represent a simplified macroscopic approach in which the porous medium is treated as a continuum. All the complexities and fine details of the microscopic pore structure are absorbed into bulk terms like permeability that reflect average properties of the medium. Semi-empirical equations such as Darcy’s

law, Blake-Kozeny-Carman or Ergun equation fall into this category. Commonly used forms of these equations are given in Table (1). Several continuum models are based in their derivation on the capillary bundle concept which will be discussed in the next section.

**Darcy's law** in its original form is a linear Newtonian model that relates the local pressure gradient in the flow direction to the fluid superficial velocity (i.e. volumetric flow rate per unit cross-sectional area) through the viscosity of the fluid and the permeability of the medium. Darcy's law is apparently the simplest model for describing the flow in porous media, and is widely used for this purpose. Although Darcy's law is an empirical relation, it can be derived from the capillary bundle model using Navier-Stokes equation via homogenization (i.e. up-scaling microscopic laws to a macroscopic scale). Different approaches have been proposed for the derivation of Darcy's law from first principles. However, theoretical analysis reveals that most of these rely basically on the momentum balance equation of the fluid phase [43]. Darcy's law is applicable to laminar flow at low Reynolds number as it contains only viscous term with no inertial term. Typically any flow with a Reynolds number less than one is laminar. As the velocity increases, the flow enters a nonlinear regime and the inertial effects are no longer negligible. The linear Darcy's law may also break down if the flow becomes vanishingly slow as interaction between the fluid and the pore walls can become important. Darcy flow model also neglects the boundary effects and heat transfer. In fact the original Darcy model neglects all effects other than viscous Newtonian effects. Therefore, the validity of Darcy's law is restricted to isothermal, purely viscous, incompressible Newtonian flow. Darcy's law has been modified differently to accommodate more complex phenomena such as non-Newtonian and multi-phase flow. Various generalizations to include nonlinearities like inertia have also been derived using homogenization or volume averaging methods [44].

Table 1: Commonly used forms of the three popular continuum models.

Model	Equation
Darcy	$\frac{\Delta P}{L} = \frac{\mu q}{K}$
Blake-Kozeny-Carman	$\frac{\Delta P}{L} = \frac{72C'\mu q(1-\epsilon)^2}{D_p^2\epsilon^3}$
Ergun	$\frac{\Delta P}{L} = \frac{150\mu q}{D_p^2} \frac{(1-\epsilon)^2}{\epsilon^3} + \frac{1.75\rho q^2}{D_p} \frac{(1-\epsilon)}{\epsilon^3}$

**Blake-Kozeny-Carman** (BKC) model for packed bed is one of the most popular models in the field of fluid dynamics to describe the flow through porous media. It encompasses a number of equations developed under various conditions and assumptions with obvious common features. This family of equations correlates the pressure drop across a granular packed bed to the superficial velocity using the fluid viscosity and the bed porosity and granule diameter. It is also used for modeling the macroscopic properties of random porous media such as permeability. These semi-empirical relations are based on the general framework of capillary bundle with various levels of sophistication. Some forms in this family envisage the bed as a bundle of straight tubes of complicated cross-section with an average hydraulic radius. Other forms depict the porous material as a bundle of tortuous tangled capillary tubes for which the equation of Navier-Stokes is applicable. The effect of tortuosity on the average velocity in the flow channels gives more accurate portrayal of non-Newtonian flow in real beds [45, 46]. The BKC model is valid for laminar flow through packed beds at low Reynolds number where kinetic energy losses caused by frequent shifting of flow channels in the bed are negligible. Empirical extension of this model to encompass transitional and turbulent flow conditions has been reported in the literature [47].

**Ergun** equation is a semi-empirical relation that links the pressure drop along a packed bed to the superficial velocity. It is widely used to portray the flow through porous materials and to model their physical properties. The input to the equation is the properties of the fluid (viscosity and mass density) and the bed (length, porosity and granule diameter). Another, and very popular, form of Ergun equation correlates the friction factor to the Reynolds number. This form is widely used for plotting experimental data and may be accused of disguising inaccuracies and defects. While Darcy and Blake-Kozeny-Carman contain only viscous term, the Ergun equation contains both viscous and inertial terms. The viscous term is dominant at low flow rates while the inertial term is dominant at high flow rates [48, 49]. As a consequence of this duality, Ergun can reach flow regimes that are not accessible to Darcy or BKC. A proposed derivation of the Ergun equation is based on a superposition of two asymptotic solutions, one for very low and one for very high Reynolds number flow. The lower limit, namely the BKC equation, is quantitatively attributable to a fully developed laminar flow in a three-dimensional porous structure, while in the higher limit the empirical Burke-Plummer equation for turbulent flow is applied [50].

The big advantage of the continuum approach is having a closed-form constitutive equation that describes the highly complex phenomenon of flow through porous media using a few simple compact terms. Consequently, the continuum models are easy to use with no computational cost. Nonetheless, the continuum approach suffers from a major limitation by ignoring the physics of flow at pore level.

Regarding non-Newtonian flow, most of these continuum models have been employed with some pertinent modification to accommodate non-Newtonian behavior. A common approach for single-phase flow is to find a suitable definition for the effective viscosity which will continue to have the dimensions and physical significance of Newtonian viscosity [51]. However, many of these attempts, theoretical and empirical, have enjoyed limited success in predicting the flow of rheologically-complex fluids in porous media. Limitations of the non-Newtonian continuum models include failure to incorporate transient time-dependent effects and to model yield-stress. Some of these issues will be examined in the coming sections.

The literature of Newtonian and non-Newtonian continuum models is overwhelming. In the following paragraph we present a limited number of illuminating examples from the non-Newtonian literature.

Darcy's law and Ergun's equation have been used by Sadowski and Bird [10, 52, 53] in their theoretical and experimental investigations to non-Newtonian flow. They applied the Ellis model to a non-Newtonian fluid flowing through a porous medium modeled by a bundle of capillaries of varying cross-sections but of a definite length. This led to a generalized form of Darcy's law and of Ergun's friction factor correlation in each of which the Newtonian viscosity was replaced by an effective viscosity. A relaxation time term was also introduced as a correction to account for viscoelastic effects in the case of polymer solutions of high molecular weight. Gogarty *et al* [54] developed a modified form of the non-Newtonian Darcy equation to predict the viscous and elastic pressure drop versus flow rate relationships for the flow of elastic carboxymethylcellulose (CMC) solutions in beds of different geometry. Park *et al* [55, 56] used the Ergun equation to correlate the pressure drop to the flow rate for a Herschel-Bulkley fluid flowing through packed beds by using an effective viscosity calculated from the Herschel-Bulkley model. To describe the non-steady flow of a yield-stress fluid in porous media, Pascal [57]

modified Darcy's law by introducing a threshold pressure gradient to account for yield-stress. This threshold gradient is directly proportional to the yield-stress and inversely proportional to the square root of the absolute permeability. Al-Fariss and Pinder [58, 59] produced a general form of Darcy's law by modifying the Blake-Kozeny equation to describe the flow in porous media of Herschel-Bulkley fluids. Chase and Dachavijit [60] modified the Ergun equation to describe the flow of yield-stress fluids through porous media using the bundle of capillary tubes approach.

### 2.1.2 Capillary Bundle Models

In the capillary bundle models the flow channels in a porous medium are depicted as a bundle of tubes. The simplest form is the model with straight, cylindrical, identical parallel tubes oriented in a single direction. Darcy's law combined with the Poiseuille's law give the following relationship for the permeability of this model

$$K = \frac{\epsilon R^2}{8} \quad (16)$$

where  $K$  and  $\epsilon$  are the permeability and porosity of the bundle respectively, and  $R$  is the radius of the tubes.

The advantage of using this simple model, rather than other more sophisticated models, is its simplicity and clarity. A limitation of the model is its disregard to the morphology of the pore space and the heterogeneity of the medium. The model fails to reflect the highly complex structure of the void space in real porous media. In fact the morphology of even the simplest medium cannot be accurately depicted by this capillary model as the geometry and topology of real void space have no similarity to a uniform bundle of tubes. The model also ignores the highly tortuous character of the flow paths in real porous media with an important impact on the flow resistance and pressure field. Tortuosity should also have consequences on the behavior of elastic and yield-stress fluids [45]. Moreover, as it is a unidirectional model its application is limited to simple one-dimensional flow situations.

One important structural feature of real porous media that is not reflected in this model is the converging-diverging nature of the pore space which has a significant influence on the flow conduct of viscoelastic and yield-stress fluids [61]. Although this simple model may be adequate for modeling some cases of slow flow

of purely viscous fluids through porous media, it does not allow the prediction of an increase in the pressure drop when used with a viscoelastic constitutive equation. Presumably, the converging-diverging nature of the flow field gives rise to an additional pressure drop, in excess to that due to shearing forces, since porous media flow involves elongational flow components. Therefore, a corrugated capillary bundle is a better choice for modeling such complex flow fields [51, 62].

Ignoring the converging-diverging nature of flow channels, among other geometrical and topological features, can also be a source of failure for this model with respect to yield-stress fluids. As a straight bundle of capillaries disregards the complex morphology of the pore space and because the yield depends on the actual geometry and connectivity not on the flow conductance, the simple bundle model will certainly fail to predict the yield point and flow rate of yield-stress fluids in porous media. An obvious failure of this model is that it predicts a universal yield point at a particular pressure drop, whereas in real porous media yield is a gradual process. Furthermore, possible bond aggregation effects due to the connectivity and size distribution of the flow paths of the porous media are completely ignored in this model.

Another limitation of this simple model is that the permeability is considered in the direction of flow only, and hence may not correctly correspond to the permeability of the porous medium especially when it is anisotropic. The model also fails to consider the pore size distributions. Though this factor may not be of relevance in some cases where the absolute permeability is of interest, it can be important in other cases such as yield-stress and certain phenomena associated with two-phase flow [63].

To remedy the flaws of the uniform bundle of tubes model and to make it more realistic, several elaborations have been suggested and used; these include

- Using a bundle of capillaries of varying cross-sections. This has been employed by Sadowski and Bird [10] and other investigators. In fact the model of corrugated capillaries is widely used especially for modeling viscoelastic flow in porous media to account for the excess pressure drop near the converging-diverging regions. The converging-diverging feature may also be used when modeling the flow of yield-stress fluids in porous media.
- Introducing an empirical tortuosity factor or using a tortuous bundle of cap-

illaries. For instance, in the Blake-Kozeny-Carman model a tortuosity factor of  $25/12$  has been used and some forms of the BKC assumes a bundle of tangled capillaries [45, 64]

- To account for the 3D flow, the model can be improved by orienting  $1/3$  of the capillaries in each of the three spatial dimensions. The permeability, as given by Equation (16), will therefore be reduced by a factor of 3 [63].
- Subjecting the bundle radius size to a statistical distribution that mimics the size distribution of the real porous media to be modeled by the bundle.

It should be remarked that the simple capillary bundle model has been targeted by heavy criticism. The model certainly suffers from several limitations and flaws as outlined earlier. However, it is not different to other models and approaches used in modeling the flow through porous media as they all are approximations with advantages and disadvantage, limitations and flaws. Like the rest, it can be an adequate model when applied within its range of validity. Another remark is that the capillary bundle model is better suited for describing porous media that are unconsolidated and have high permeability [65]. This seems in line with the previous remark as the capillary bundle is an appropriate model for this relatively simple porous medium with comparatively plain structure.

Capillary bundle models have been widely used in the investigation of Newtonian and non-Newtonian flow through porous media with various levels of success. Past experience, however, reveals that no single capillary model can be successfully applied in diverse structural and rheological situations. The capillary bundle should therefore be designed and used with reference to the situation in hand. Because the capillary bundle models are the basis for most continuum models, as the latter usually rely in their derivation on some form of capillary models, most of the previous literature on the use of the continuum approach applies to the capillary bundle. Here, we give a short list of some contributions in this field in the context of non-Newtonian flow.

Sadowski [52, 53] applied the Ellis rheological model to a corrugated capillary model of a porous medium to derive a modified Darcy's law. Park [56] used a capillary model in developing a generalized scale-up method to adapt Darcy's law to non-Newtonian fluids. Al-Fariss and Pinder [66] extended the capillary bundle model to the Herschel-Bulkley fluids and derived a form of the BKC model for

yield-stress fluid flow through porous media at low Reynolds number. Vradis and Protopapas [67] extended a simple capillary tubes model to describe the flow of Bingham fluids in porous media and presented a solution in which the flow is zero below a threshold head gradient and Darcian above it. Chase and Dachavijit [60] also applied the bundle of capillary tubes approach to model the flow of a yield-stress fluid through a porous medium, similar to the approach of Al-Fariss and Pinder.

### 2.1.3 Numerical Methods

In the numerical approach, a detailed description of the porous medium at pore-scale with the relevant physics at this level is used. To solve the flow field, numerical methods, such as finite volume and finite difference, usually in conjunction with computational implementation are utilized. The advantage of the numerical methods is that they are the most direct way to describe the physical situation and the closest to full analytical solution. They are also capable, in principle at least, to deal with time-dependent transient situations. The disadvantage is that they require a detailed pore space description. Moreover, they are very complex and hard to implement with a huge computational cost and serious convergence difficulties. Due to these complexities, the flow processes and porous media that are currently within the reach of numerical investigation are the most simple ones. These methods are also in use for investigating the flow in capillaries with various geometries as a first step for modeling the flow in porous media and the effect of corrugation on the flow field.

In the following we present a brief look with some examples from the literature for using numerical methods to investigate the flow of non-Newtonian fluids in porous media. In many cases the corrugated capillary was used to model the converging-diverging nature of the passages in real porous media.

Talwar and Khomami [68] developed a higher order Galerkin finite element scheme for simulating a two-dimensional viscoelastic flow and tested the algorithm on the flow of Upper Convected Maxwell (UCM) and Oldroyd-B fluids in undulating tube. It was subsequently used to solve the problem of transverse steady flow of these two fluids past an infinite square arrangement of infinitely long, rigid, motionless cylinders. Souvaliotis and Beris [69] developed a domain decomposition spectral collocation method for the solution of steady-state, nonlinear viscoelastic

flow problems. The method was then applied to simulate viscoelastic flows of UCM and Oldroyd-B fluids through model porous media represented by a square array of cylinders and a single row of cylinders. Hua and Schieber [70] used a combined finite element and Brownian dynamics technique (CONNFESSIT) to predict the steady-state viscoelastic flow field around an infinite array of square-arranged cylinders using two kinetic theory models. Fadili *et al* [71] derived an analytical 3D filtration formula for up-scaling isotropic Darcy's flows of power-law fluids to heterogeneous Darcy's flows by using stochastic homogenization techniques. They then validated their formula by making a comparison with numerical experiments for 2D flows through a rectangular porous medium using finite volume method.

Concerning the non-uniformity of flow channels and its impact on the flow which is an issue related to the flow through porous media, numerical techniques have been used by a number of researchers to investigate the flow of viscoelastic fluids in converging-diverging geometries. For example, Deiber and Schowalter [13, 72] used the numerical technique of geometric iteration to solve the nonlinear equations of motion for viscoelastic flow through tubes with sinusoidal axial variations in diameter. Pilitsis *et al* [73] carried a numerical simulation to the flow of a shear-thinning viscoelastic fluid through a periodically constricted tube using a variety of constitutive rheological models. Momeni-Masuleh and Phillips [74] used spectral methods to investigate viscoelastic flow in an undulating tube.

#### 2.1.4 Pore-Scale Network Modeling

The field of network modeling is too diverse and complex to be fairly presented in this article. We therefore present a general background on this subject followed by a rather detailed account of one of the network models as an example. This is the model developed by a number of researchers at Imperial College London [75–77]. One reason for choosing this example is because it is a well developed model that incorporates the main features of network modeling in its current state. Moreover, it produced some of the best results in this field when compared to the available theoretical models and experimental data. Because of the nature of this article, we will focus on the single-phase non-Newtonian aspects.

Pore-scale network modeling is a relatively novel method that have been developed to deal with the flow through porous media and other related issues. It can be seen as a compromise between the two extremes of continuum and numerical

approaches as it partly accounts for the physics of flow and void space structure at pore level with affordable computational resources. Network modeling can be used to describe a wide range of properties from capillary pressure characteristics to interfacial area and mass transfer coefficients. The void space is described as a network of flow channels with idealized geometry. Rules that determine the transport properties in these channels are incorporated in the network to compute effective properties on a mesoscopic scale. The appropriate pore-scale physics combined with a representative description of the pore space gives models that can successfully predict average behavior [78, 79].

Various network modeling methodologies have been developed and used. The general feature is the representation of the pore space by a network of interconnected ducts (bonds or throats) of regular shape and the use of a simplified form of the flow equations to describe the flow through the network. A numerical solver is usually employed to solve a system of simultaneous equations to determine the flow field. The network can be two-dimensional or three-dimensional with a random or regular lattice structure such as cubic. The shape of the cylindrical ducts include circular, square and triangular cross section (possibly with different shape factor) and may include converging-diverging feature. The network elements may contain, beside the conducting ducts, nodes (pores) that can have zero or finite volume and may well serve a function in the flow phenomena or used as junctions to connect the bonds. The simulated flow can be Newtonian or non-Newtonian, single-phase, two-phase or even three-phase. The physical properties of the flow and porous medium that can be obtained from flow simulation include absolute and relative permeability, formation factor, resistivity index, volumetric flow rate, apparent viscosity, threshold yield pressure and much more. Typical size of the network is a few millimeters. One reason for this minute size is to reduce the computational cost. Another reason is that this size is sufficient to represent a homogeneous medium having an average throat size of the most common porous materials. Up-scaling the size of a network is a trivial task if larger pore size is required. Moreover, extending the size of a network model by attaching identical copies of the same model in any direction or imposing repeated boundary conditions is another simple task [78, 80–83].

The general strategy in network modeling is to use the bulk rheology of the fluid and the void space description of the porous medium as an input to the model. The flow simulation in a network starts by modeling the flow in a single capillary.

The flow in a single capillary can be described by the following general relation

$$Q = G' \Delta P \quad (17)$$

where  $Q$  is the volumetric flow rate,  $G'$  is the flow conductance and  $\Delta P$  is the pressure drop. For a particular capillary and a specific fluid,  $G'$  is given by

$$\begin{aligned} G' &= G'(\mu) = \text{constant} && \text{Newtonian fluid} \\ G' &= G'(\mu, \Delta P) && \text{Purely viscous non-Newtonian fluid} \\ G' &= G'(\mu, \Delta P, t) && \text{Fluid with memory} \end{aligned} \quad (18)$$

For a network of capillaries, a set of equations representing the capillaries and satisfying mass conservation have to be solved simultaneously to find the pressure field and other physical quantities. A numerical solver is usually employed in this process. For a network with  $n$  nodes there are  $n$  equations in  $n$  unknowns. These unknowns are the pressure values at the nodes. The essence of these equations is the continuity of flow of incompressible fluid at each node in the absence of sources and sinks. To find the pressure field, this set of equations have to be solved subject to the boundary conditions which are the pressures at the inlet and outlet of the network. This unique solution is ‘consistent’ and ‘stable’ as it is the only mathematically acceptable solution to the problem, and, assuming the modeling process and the mathematical technicalities are reliable, should mimic the unique physical reality of the pressure field in the porous medium.

For Newtonian fluid, a single iteration is needed to solve the pressure field as the flow conductance is known in advance because the viscosity is constant. For purely viscous non-Newtonian fluid, the process starts with an initial guess for the viscosity, as it is unknown and pressure-dependent, followed by solving the pressure field iteratively and updating the viscosity after each iteration cycle until convergence is reached. For memory fluids, the dependence on time must be taken into account when solving the pressure field iteratively. Apparently, there is no general strategy to deal with this situation. However, for the steady-state flow of memory fluids of elastic nature a sensible approach is to start with an initial guess for the flow rate and iterate, considering the effect of the local pressure and viscosity variation due to converging-diverging geometry, until convergence is achieved. This approach was presented by Tardy and Anderson [32] and implemented with some adaptation by Sochi [77].

With regards to modeling the flow in porous media of complex fluids that have time dependency in a dynamic sense due to thixotropic or elastic nature, there are three major difficulties

- The difficulty of tracking the fluid elements in the pores and throats and identifying their deformation history, as the path followed by these elements is random and can have several unpredictable outcomes.
- The mixing of fluid elements with various deformation history in the individual pores and throats. As a result, the viscosity is not a well-defined property of the fluid in the pores and throats.
- The change of viscosity along the streamline since the deformation history is continually changing over the path of each fluid element.

These complications can be ignored when dealing with cases of steady-state flow. Some suggestions on network modeling of time-dependent thixotropic flow will be presented in Section (5).

Despite all these complications, network modeling in its current state is a simplistic approach that models the flow in ideal situations. Most network models rely on various simplifying assumptions and disregard important physical processes that have strong influence on the flow. One such simplification is the use of geometrically uniform network elements to represent the flow channels. Viscoelasticity and yield-stress are among the physical processes that are compromised by this idealization of void space. Another simplification is the dissociation of the various flow phenomena. For example, in modeling the flow of yield-stress fluids through porous media an implicit assumption is usually made that there is no time dependency or viscoelasticity. This assumption, however, can be reasonable in the case of modeling the dominant effect and may be valid in practical situations where other effects are absent or insignificant. A third simplification is the adoption of no-slip-at-wall condition. This widely accepted assumption means that the fluid at the boundary is stagnant relative to the solid boundary. The effect of slip, which includes reducing shear-related effects and influencing yield-stress behavior, is very important in certain circumstances and cannot be ignored. However, this assumption is not far from reality in many other situations. Furthermore, wall roughness, which is the rule in porous media, usually prevents wall slip or reduces its effect. Other physical phenomena that can be incorporated in the network models to make it more

realistic include retention (e.g. by adsorption or mechanical trapping) and wall exclusion. Most current network models do not take account of these phenomena.

The Imperial College model [75–77], which we present here as an example, uses three-dimensional networks built from a topologically-equivalent three-dimensional voxel image of the pore space with the pore sizes, shapes and connectivity reflecting the real medium. Pores and throats are modeled as having triangular, square or circular cross-section by assigning a shape factor which is the ratio of the area to the perimeter squared and obtained from the pore space image. Most of the network elements are not circular. To account for the non-circularity when calculating the volumetric flow rate analytically or numerically for a cylindrical capillary, an equivalent radius  $R_{eq}$  is used

$$R_{eq} = \left( \frac{8G}{\pi} \right)^{1/4} \quad (19)$$

where the geometric conductance,  $G$ , is obtained empirically from numerical simulation. The network can be extracted from voxel images of a real porous material or from voxel images generated by simulating the geological processes by which the porous medium was formed. Examples for the latter are the two networks of Statoil which represent two different porous media: a sand pack and a Berea sandstone. These networks are constructed by Øren and coworkers [84, 85] and are used by several researchers in flow simulation studies. Another possibility for generating a network is by employing computational algorithms based on numeric statistical data extracted from the porous medium of interest. Other possibilities can also be found in the literature.

Assuming a laminar, isothermal and incompressible flow at low Reynolds number, the only equations that require attention are the constitutive equation for the particular fluid and the conservation of volume as an expression for the conservation of mass. For Newtonian flow, the pressure field can be solved once and for all. For non-Newtonian flow, the situation is more complex as it involves non-linearities and requires iterative techniques. For the simplest case of time-independent fluids, the strategy is to start with an arbitrary guess. Because initially the pressure drop in each network element is not known, an iterative method is used. This starts by assigning an effective viscosity  $\mu_e$  to the fluid in each network element. The effective viscosity is defined as that viscosity which makes Poiseuille’s equation fits any set of laminar flow conditions for time-independent fluids [1]. By invoking the

conservation of volume for incompressible fluid, the pressure field across the entire network is solved using a numerical solver [86]. Knowing the pressure drops in the network, the effective viscosity of the fluid in each element is updated using the expression for the flow rate with the Poiseuille's law as a definition. The pressure field is then recomputed using the updated viscosities and the iteration continues until convergence is achieved when a specified error tolerance in the total flow rate between two consecutive iteration cycles is reached. Finally, the total volumetric flow rate and the apparent viscosity, defined as the viscosity calculated from the Darcy's law, are obtained.

For the steady-state flow of viscoelastic fluids, the approach of Tardy and Anderson [32, 77] was used as outlined below

- The capillaries of the network are modeled with contraction to account for the effect of converging-diverging geometry on the flow. The reason is that the effects of fluid memory take place on going through a radius change, as this change induces a change in strain rate with a consequent viscosity changing effects. Examples of the converging-diverging geometries are given in Figure (9).
- Each capillary is discretized in the flow direction and a discretized form of the flow equations is used assuming a prior knowledge of the stress and viscosity at the inlet of the network.
- Starting with an initial guess for the flow rate and using iterative technique, the pressure drop as a function of the flow rate is found for each capillary.
- Finally, the pressure field for the whole network is found iteratively until convergence is achieved. Once this happens, the flow rate through each capillary in the network can be computed and the total flow rate through the network is determined by summing and averaging the flow through the inlet and outlet capillaries.

For yield-stress fluids, total blocking of the elements below their threshold yield pressure is not allowed because if the pressure have to communicate, the substance before yield should be considered a fluid with high viscosity. Therefore, to simulate the state of the fluid before yield the viscosity is set to a very high but finite value so the flow virtually vanishes. As long as the yield-stress substance is assumed to

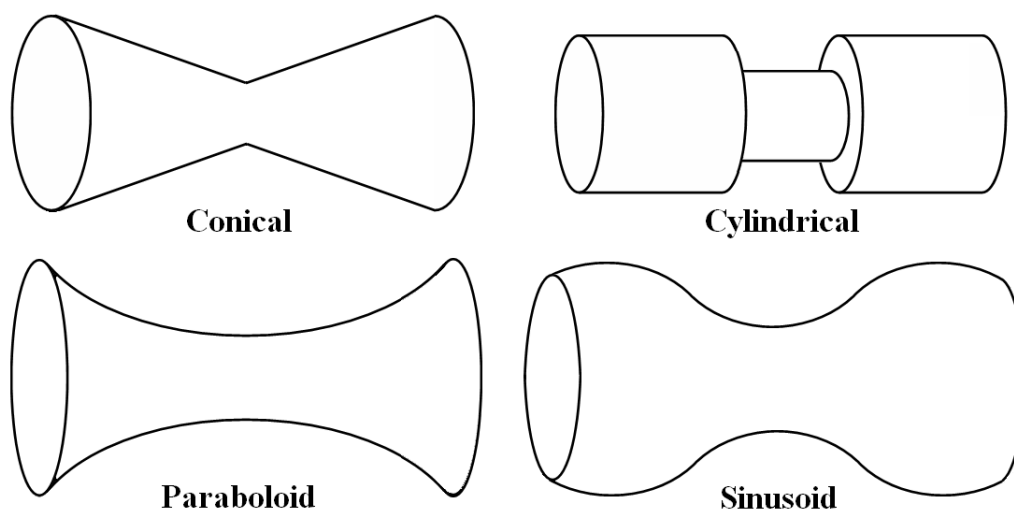


Figure 9: Examples of corrugated capillaries that can be used to model converging-diverging geometry in porous media.

be fluid, the pressure field will be solved as for non-yield-stress fluids because the situation will not change fundamentally by the high viscosity. It is noteworthy that the assumption of very high but finite zero-stress viscosity for yield-stress fluids is realistic and supported by experimental evidence. A further condition is imposed before any element is allowed to yield, that is the element must be part of a non-blocked path spanning the network from the inlet to the outlet. What necessitates this condition is that any conducting element should have a source on one side and a sink on the other, and this will not happen if either or both sides are blocked.

Finally, a brief look at the literature of network modeling of non-Newtonian flow through porous media will provide better insight into this field and its contribution to the subject. In their investigation to the flow of shear-thinning fluids in porous media, Sorbie *et al* [63, 87] used 2D network models made up of connected arrays of capillaries to represent the porous medium. The capillaries were placed on a regular rectangular lattice aligned with the principal direction of flow, with constant bond lengths and coordination number 4, but the tube radii are picked from a random distribution. The non-Newtonian flow in each network element was described by the Carreau model. Coombe *et al* [88] used a network modeling approach to analyze the impact of the non-Newtonian flow characteristics of polymers, foams, and emulsions at three lengths and time scales. They employed a reservoir simulator to create networks of varying topology in order to study the impact of porous media structure on rheological behavior. Shah *et al* [89] used small size 2D networks to

study immiscible displacement in porous media involving power-law fluids. Their pore network simulations include drainage where a power-law fluid displaces a Newtonian fluid at a constant flow rate, and the displacement of one power-law fluid by another with the same power-law index. Tian and Yao [90] used network models of cylindrical capillaries on a 2D square lattice to study immiscible displacements of two-phase non-Newtonian fluids in porous media. In this investigation the injected and the displaced fluids are considered as Newtonian and non-Newtonian Bingham fluids respectively.

To study the flow of power-law fluids through porous media, Pearson and Tardy [51] employed a 2D square-grid network of capillaries, where the radius of each capillary is randomly distributed according to a predefined probability distribution function. Their investigation included the effect of the rheological and structural parameters on the non-Newtonian flow behavior. Tsakiroglou [91, 92] and Tsakiroglou *et al* [93] used pore network models on 2D square lattices to investigate various aspects of single- and two-phase flow of non-Newtonian fluids in porous media. The rheological models which were employed in this investigation include Meter, power-law and mixed Meter and power-law. Lopez *et al* [76, 94, 95] investigated single- and two-phase flow of shear-thinning fluids in porous media using network modeling. They used morphologically complex 3D networks to model the porous media, while the shear-thinning rheology was described by Carreau model. Balhoff and Thompson [96–98] employed 3D random network models extracted from computer-generated random sphere packing to investigate the flow of shear-thinning and yield-stress fluids in packed beds. The power-law, Ellis and Herschel-Bulkley fluids were used as rheological models. To model non-Newtonian flow in the throats, they used analytical expressions for a capillary tube with empirical tuning to key parameters to represent the throat geometry and simulate the fluid dynamics. Perrin *et al* [99] used network modeling with Carreau rheology to analyze their experimental findings on the flow of hydrolyzed polyacrylamide solutions in etched silicon micromodels. The network simulation was performed on a 2D network model with a range of rectangular channel widths exactly as in the physical micromodel experiment. Sochi and Blunt [12, 77] used network modeling to study single-phase non-Newtonian flow in porous media. Their investigation includes modeling the Ellis and Herschel-Bulkley as time-independent rheological models and the Bautista-Manero as a viscoelastic model with thixotropic features. The non-Newtonian phenomena that can be described by these models include shear-thinning, shear-thickening, yield-stress, thixotropy and viscoelasticity.

Network modeling was also used by several researchers to investigate the generation and mobilization of foams and yield-stress fluids in porous media. These include Rossen and Mamun [100] and Chen *et al* [101–103].

### 3 Yield-Stress

Yield-stress or viscoplastic fluids are characterized by their ability to sustain shear stresses, that is a certain amount of stress must be exceeded before the flow initiates. So an ideal yield-stress fluid is a solid before yield and a fluid after. Accordingly, the viscosity of the substance changes from an infinite to a finite value. However, the physical situation indicates that it is more realistic to regard a yield-stress substance as a fluid whose viscosity as a function of applied stress has a discontinuity as it drops sharply from a very high value on exceeding a critical stress. There are many controversies and unsettled issues in the non-Newtonian literature about yield-stress phenomenon and yield-stress fluids. In fact, even the concept of a yield-stress has received much recent criticism, with evidence presented to suggest that most materials weakly yield or creep near zero strain rate. The supporting argument is that any material will flow provided that one waits long enough. These conceptual difficulties are backed by practical and experimental complications. For example, the value of yield-stress for a particular fluid is difficult to measure consistently and it may vary by more than an order of magnitude depending on the measurement technique. Several constitutive equations to describe liquids with yield-stress are in use; the most popular ones are Bingham, Casson and Herschel-Bulkley. Some have suggested that the yield-stress values obtained via such models should be considered model parameters and not real material properties [6, 9, 27, 104, 105].

There are several difficulties in working with yield-stress fluids and validating the experimental data. One difficulty is that yield-stress value is usually obtained by extrapolating a plot of shear stress to zero shear rate [9, 55, 58]. This can result in a variety of values for yield-stress, depending on the distance from the shear stress axis experimentally accessible by the instrument used. The vast majority of yield-stress data reported results from such extrapolations, making most values in the literature instrument-dependent [9]. Another method used to measure yield-stress is by lowering the shear rate until the shear stress approaches a constant. This may be described as the dynamic yield-stress [17]. The results obtained using such methods may not agree with the static yield-stress measured directly without disturbing the microstructure during the measurement. The latter seems more relevant to the flow initiation under gradual increase in pressure gradient as in the case of flow in porous media. Consequently, the accuracy of the predictions made using flow simulation models in conjunction with such experimental data is limited.

Another difficulty is that while in the case of pipe flow the yield-stress value is a property of the fluid, in the case of flow in porous media there are strong indications that in a number of situations it may depend on both the fluid and the porous medium itself [67, 106]. One possible explanation is that yield-stress value may depend on the size and shape of the pore space when the polymer molecules become comparable in size to the pore. The implicit assumption that yield-stress value at pore-scale is the same as the value at bulk may not be self evident. This makes the predictions of the models based on analytical solution to the flow in a uniformly-shaped tube combined with the bulk rheology less accurate. When the duct size is small, as it is usually the case in porous media, flow of macromolecule solutions normally displays deviations from predictions based on corresponding viscometric data [107]. Moreover, the highly complex shape of flow paths in porous media must have a strong impact on the actual yield point, and this feature is lost by modeling these paths with ducts of idealized geometry. Consequently, the concept of equivalent radius  $R_{eq}$ , which is used in network modeling, though is completely appropriate for Newtonian fluids and reasonably appropriate for purely viscous non-Newtonian fluids with no yield-stress, seems inappropriate for yield-stress fluids as yield depends on the actual shape of the void space rather than the equivalent radius and flow conductance.

### 3.1 Modeling Yield-Stress in Porous Media

In this section we outline the failure of the four approaches for modeling the flow through porous media in dealing with the flow of yield-stress fluids. It is apparent that no continuum model can predict the yield point of a yield-stress fluid in complex porous media. The reason is that these models do not account for the complex geometry and topology of the void space. As the yield point depends on the fine details of the pore space structure, no continuum model is expected to predict the threshold yield pressure (TYP) of yield-stress fluids in porous media. The continuum models also fail to predict the flow rate, at least at transition stage where the medium is partly conducting, because according to these models the medium is either fully blocked or fully flowing whereas in reality the yield of porous medium is a gradual process.

Regarding the capillary bundle models, the situation is similar to the continuum models as they predict a single universal yield if a uniform bundle of capillaries is assumed. Moreover, because all capillary bundle models fail to capture the

topology and geometry of complex porous media they cannot predict the yield point and describe the flow rate of yield-stress fluids in porous media since yield is highly dependent on the fine details of the void space. An important aspect of the geometry of real porous media which strongly affects the yield point and flow rate of yield-stress fluids is the converging-diverging nature of the flow paths. This feature is not reflected by the bundle of uniform capillaries models. Another feature is the connectivity of the flow channels where bond aggregation (i.e. how the throats are distributed and arranged) strongly affects yield behavior.

Concerning the application of numerical methods to yield-stress fluids in porous media, very few studies can be found on this subject (e.g. [108]). Moreover, the results, which are reported only for very simple cases of porous media, cannot be fully assessed. It seems therefore that network modeling is the only viable candidate for modeling yield-stress fluids in porous media. However, because the research in this field is limited, no final conclusion on the merit of this approach can be reached. Nonetheless, the modest success in modeling yield-stress as experienced by some investigators (e.g. Balhoff [98] and Sochi [77, 105]) indicates that network modeling in its current state is not capable of dealing with such a complex phenomenon. One possible reason is the comparative simplicity of the rheological models, such as Bingham, used in these investigations. These models can possibly offer a phenomenological description of yield-stress in simple flow situations but are certainly unable to accommodate the underlying physics at pore level in complex porous media. Consequently, yield-stress as a model parameter obtained in bulk viscometry may not be appropriate to use in this complex situation. Another reason is the experimental difficulties associated with yield-stress fluids. This can make the experimental results subject to complications, such as viscoelasticity and retention, that may not be accounted for in the network model. A third reason is the relative simplicity of the current network modeling approach to yield-stress fluids. This is supported by the fact that better results are usually obtained for non-yield-stress fluids using the same network modeling techniques. One major limitation of the current network models with regard to yield-stress fluids is the use of analytical expressions for cylindrical tubes based on the concept of equivalent radius  $R_{eq}$ . This is far from reality where the void space retains highly complex shape and connectivity. Consequently, the yield condition for cylindrical capillaries becomes invalid approximation to the yield condition for the intricate flow paths in porous media.

In summary, yield-stress fluid results are extremely sensitive to how the fluid is characterized, how the void space is described and how the yield process is modeled. In the absence of a comprehensive and precise incorporation of all these factors in the network model, pore-scale modeling of yield-stress fluids in porous media remains a crude approximation that may not produce quantitatively sensible predictions. The final conclusion is that yield-stress is a problematic phenomenon, and hence very modest success has been achieved in this area by any one of the four modeling approaches.

## 3.2 Predicting Threshold Yield Pressure (TYP)

Here we discuss the attempts to predict the yield point of a complex porous medium from the void space description and yield-stress value of an ideal yield-stress fluid without modeling the flow process. In the literature of yield-stress we can find two well-developed methods proposed for predicting the yield point of a morphologically-complex network that depicts a porous medium; these are the Minimum Threshold Path (MTP) and the percolation theory. In this regard, there is an implicit assumption that the network is an exact replica of the medium and the yield-stress value reflects the yield-stress of real fluid so that any failure of these algorithms can not be attributed to mismatch or any factor other than flaws in these algorithms. It should be remarked that the validity of these methods can be tested by experiment [103, 109].

### 3.2.1 Minimum Threshold Path Approach

Predicting the threshold yield pressure of a yield-stress fluid in porous media in its simplest form may be regarded as a special case of the more general problem of finding the threshold conducting path in disordered media that consist of elements with randomly distributed thresholds. This problem was analyzed by Roux and Hansen [110] in the context of studying the conduction of an electric network of diodes by considering two different cases, one in which the path is directed (no backtracking) and one in which it is not. They suggested that the minimum overall threshold potential difference across the network is akin to a percolation threshold and investigated its dependence on the lattice size. Kharabaf and Yortsos [111] noticed that a firm connection of the lattice-threshold problem to percolation appears to be lacking and the relation of the Minimum Threshold Path (MTP) to the minimum

path of percolation, if it indeed exists, is not self-evident. They presented a new algorithm, Invasion Percolation with Memory (IPM), for the construction of the MTP, based on which its properties can be studied. The Invasion Percolation with Memory method was further extended by Chen *et al* [103] to incorporate dynamic effects due to viscous friction following the onset of mobilization [102, 112–116].

The IPM is an algorithm for finding the inlet-to-outlet path that minimizes the sum of values of a property assigned to the individual elements of the network, and hence finding this minimum. For a yield-stress fluid, this reduces to finding the inlet-to-outlet path that minimizes the yield pressure. The yield pressure of this path is then taken as the network threshold yield pressure. A detailed description of this algorithm is given in [77, 111]. Other algorithms that achieve this minimization process can be found in the literature. However, they all rely on a similar assumption to that upon which the IPM is based, that is the threshold yield pressure of a network is the minimum sum of the threshold yield pressures of the individual elements of all possible paths from the inlet to the outlet.

There are two possibilities for defining yield stress fluids before yield: either solid-like substances or liquids with very high viscosity. According to the first, the most sensible way for modeling a presumed pressure gradient inside a medium is to be a constant, that is the pressure drop across the medium is a linear function of the spatial coordinate in the flow direction, as any other assumption needs justification. Whereas in the second case the fluid should be treated like non-yield-stress fluids and hence the pressure field inside the porous medium should be subject to the consistency criterion for the pressure field which was introduced earlier. The logic is that the magnitude of the viscosity should have no effect on the flow conduct as long as the material is assumed to be fluid.

Several arguments can be presented against the MTP algorithms for predicting the yield point of a medium or a network. Though certain arguments may be more obvious for a network with cylindrical ducts, they are valid in general for regular and irregular geometries of flow channels. Some of these arguments are outlined below

- The MTP algorithms are based on the assumption that the threshold yield pressure (TYP) of an ensemble of serially connected bonds is the sum of their yield pressures. This assumption can be challenged by the fact that for a non-uniform ensemble (i.e. an ensemble whose elements have different

TYPs) the pressure gradient across the ensemble should reach the threshold yield gradient of the bottleneck (i.e. the element with the highest TYP) of the ensemble if yield should occur. Consequently, the TYP of the ensemble will be higher than the sum of the TYPs of the individual elements. This argument may be more obvious if yield-stress fluids are regarded as solids and a linear pressure drop is assumed.

- Assuming the yield-stress substances before yield are fluids with high viscosity, the dynamic aspects of the pressure field are neglected because the aim of the MTP algorithms is to find a collection of bonds inside the network with a certain condition based on the intrinsic properties of these elements irrespective of the pressure field. The reality is that the bonds are part of a network that is subject to a pressure field, so the pressure across each individual element must comply with a dynamically stable pressure configuration over the whole network. The MTP algorithms rely for justification on a hidden assumption that the minimum sum condition is identical or equivalent to the stable configuration condition, which is not obvious, because it is very unlikely that a stable configuration will require a pressure drop across each element of the path of minimum sum that is identical to the threshold yield pressure of that element. Therefore, it is not clear that the actual path of yield must coincide, totally or partially, with the path of the MTP algorithms let alone that the actual value of yield pressure must be predicted by these methods. To sum up, these algorithms disregard the global pressure field which can communicate with the internal nodes of the serially connected ensemble as it is part of a network and not an isolated collection of bonds. It is not obvious that the condition of these algorithms should agree with the requirement of a stable and mathematically consistent pressure field as defined in Section (2.1). Such an agreement should be regarded as an extremely unlikely coincidence.
- The MTP algorithms that allows backtracking have another drawback that is in some cases the path of minimum sum requires a physically unacceptable pressure configuration. This may be more obvious if the yield-stress substances are assumed to be solid before yield though it is still valid with the fluid assumption.
- The effect of tortuosity is ignored since it is implicitly assumed that the path of yield is an ensemble of serially-connected and linearly-aligned tubes,

whereas in reality the path is generally tortuous as it is part of a network and can communicate with the global pressure field through the intermediate nodes. The effect of tortuosity, which is more obvious for the solid assumption, is a possible increase in the external threshold pressure gradient and a possible change in the bottleneck.

### 3.2.2 Percolation Theory Approach

Percolation theory is a mathematical branch that deals with ensembles of connected elements with a common particular property. The objective is to quantify the probabilistic percolation threshold in these random systems and identify the percolation paths based on the intrinsic properties of these elements. There are many scientific applications to this huge and rapidly growing subject. These include the flow of fluids through porous media and random networks of capillaries, and the electric conductivity of a network of electric components such as resistors and diodes [117–121].

Concerning the percolation approach, it is tempting to consider the conduct of yield-stress fluids in porous media as a percolation phenomenon to be analyzed by the classical percolation theory. However, three reasons, at least, may suggest otherwise

1. The conventional percolation models can be applied only if the conducting elements are homogeneous, i.e. it is assumed in these models that the intrinsic property of all elements in the network are equal. However, this assumption cannot be justified for most kinds of media where the elements vary in their conduction and yield properties. Therefore, to apply percolation principles, a generalization to the conventional percolation theory is needed as suggested by Selyakov and Kadet [117].
2. The network elements cannot yield independently as a spanning path bridging the inlet to the outlet is a necessary condition for yield. This contradicts the percolation theory assumption that the elements conduct independently.
3. The pure percolation approach ignores the dynamic aspects of the pressure field, that is a stable pressure configuration is a necessary condition which may not coincide with the simple percolation requirement. The percolation

condition, as required by the classic percolation theory, determines the stage at which the network starts flowing according to the intrinsic properties of its elements as an ensemble of conducting bonds regardless of the dynamic aspects introduced by the external pressure field. This argument is more obvious if yield-stress substances are regarded as fluids with high viscosity.

In a series of studies on generation and mobilization of foam in porous media, Rossen *et al* [100, 122] analyzed the threshold yield pressure using percolation theory concepts and suggested a simple percolation model. In this model, the percolation cluster is first found, then the MTP was approximated as a subset of this cluster that samples those bonds with the smallest individual thresholds [103]. This approach relies on the validity of applying percolation theory to yield-stress, which is disputed. Moreover, it is a mere coincidence if the yield path is contained within the percolation sample. Yield is an on/off process which critically depends on factors other than smallness of individual thresholds. These factors include the particular distribution and configuration of these elements, being within a larger network and hence being able to communicate with the global pressure field, and the dynamic aspects of the pressure field and stability requirement. Any approximation, therefore, has very little meaning in this context.

## 4 Viscoelasticity

Viscoelastic substances exhibit a dual nature of behavior by showing signs of both viscous fluids and elastic solids. In its most simple form, viscoelasticity can be modeled by combining Newton's law for viscous fluids (stress  $\propto$  rate of strain) with Hook's law for elastic solids (stress  $\propto$  strain), as given by the original Maxwell model and extended by the Convected Maxwell models for the nonlinear viscoelastic fluids. Although this idealization predicts several basic viscoelastic phenomena, it does so only qualitatively. The behavior of viscoelastic fluids is drastically different from that of Newtonian and inelastic non-Newtonian fluids. This includes the presence of normal stresses in shear flows, sensitivity to deformation type, and memory effects such as stress relaxation and time-dependent viscosity. These features underlie the observed peculiar viscoelastic phenomena such as rod-climbing (Weissenberg effect), die swell and open-channel siphon [18]. Most viscoelastic fluids exhibit shear-thinning and an elongational viscosity that is both strain and extensional strain rate dependent, in contrast to Newtonian fluids where the elongational viscosity is constant and in proportion to shear viscosity [28].

The behavior of viscoelastic fluids at any time is dependent on their recent deformation history, that is they possess a fading memory of their past. Indeed a material that has no memory cannot be elastic, since it has no way of remembering its original shape. Consequently, an ideal viscoelastic fluid should behave as an elastic solid in sufficiently rapid deformations and as a Newtonian liquid in sufficiently slow deformations. The justification is that the larger the strain rate, the more strain is imposed on the sample within the memory span of the fluid [6, 18, 28]. Many materials are viscoelastic but at different time scales that may not be reached. Dependent on the time scale of the flow, viscoelastic materials show mainly viscous or elastic behavior. The particular response of a sample in a given experiment depends on the time scale of the experiment in relation to a natural time of the material. Thus, if the experiment is relatively slow, the sample will appear to be viscous rather than elastic, whereas, if the experiment is relatively fast, it will appear to be elastic rather than viscous. At intermediate time scales mixed viscoelastic response is observed. Therefore the concept of a natural time of a material is important in characterizing the material as viscous or elastic. The ratio between the material time scale and the time scale of the flow is indicated by a non-dimensional number: the Deborah or the Weissenberg number [7].

A common feature of viscoelastic fluids is stress relaxation after a sudden shearing displacement where stress overshoots to a maximum then starts decreasing exponentially and eventually settles to a steady-state value. This phenomenon also takes place on cessation of steady shear flow where stress decays over a finite measurable length of time. This reveals that viscoelastic fluids are able to store and release energy in contrast to inelastic fluids which react instantaneously to the imposed deformation [6, 13, 18]. A defining characteristic of viscoelastic materials associated with stress relaxation is the relaxation time which may be defined as the time required for the shear stress in a simple shear flow to return to zero under constant strain condition. Hence for a Hookean elastic solid the relaxation time is infinite, while for a Newtonian fluid the relaxation of the stress is immediate and the relaxation time is zero. Relaxation times which are infinite or zero are never realized in reality as they correspond to the mathematical idealization of Hookean elastic solids and Newtonian liquids. In practice, stress relaxation after the imposition of constant strain condition takes place over some finite non-zero time interval [3].

The complexity of viscoelasticity is phenomenal and the subject is notorious for being extremely difficult and challenging. The constitutive equations for viscoelastic fluids are much too complex to be treated in a general manner. Further complications arise from the confusion created by the presence of other phenomena such as wall effects and polymer-wall interactions, and these appear to be system specific [123]. Therefore, it is doubtful that a general fluid model capable of predicting all the flow responses of viscoelastic systems with enough mathematical simplicity or tractability can emerge in the foreseeable future [13, 47, 124]. Understandably, despite the huge amount of literature composed in the last few decades on this subject, the overwhelming majority of these studies have investigated very simple cases in which substantial simplifications have been made using basic viscoelastic models.

In the last few decades, a general consensus has emerged that in the flow of viscoelastic fluids through porous media elastic effects should arise, though their precise nature is unknown or controversial. In porous media, viscoelastic effects can be important in certain cases. When they are, the actual pressure gradient will exceed the purely viscous gradient beyond a critical flow rate, as observed by several investigators. The normal stresses of high molecular polymer solutions can explain in part the high flow resistance encountered during viscoelastic flow

through porous media. It is believed that the very high normal stress differences and Trouton ratios associated with polymeric fluids will produce increasing values of apparent viscosity when the flow channels in the porous medium are of rapidly changing cross section.

Important aspects of non-Newtonian flow in general and viscoelastic flow in particular through porous media are still presenting serious challenge for modeling and quantification. There are intrinsic difficulties in characterizing non-Newtonian effects in the flow of polymer solutions and the complexities of the local geometry of the porous medium. This geometry gives rise to a complex and pore space dependent flow field in which shear and extension coexist in various proportions that cannot be quantified. Flows through porous media cannot be classified as pure shear flows as the converging-diverging passages impose a predominantly extensional flow fields especially at high flow rates. The extension viscosity of many non-Newtonian fluids also increases dramatically with the extension rate. As a consequence, the relationship between the pressure drop and flow rate very often do not follow the observed Newtonian and inelastic non-Newtonian trend. Further complications arise from the fact that for complex fluids the stress depends not only on whether the flow is a shearing, extensional, or mixed type, but also on the whole history of the velocity gradient [17, 51, 125–129].

## 4.1 Important Aspects for Flow in Porous Media

Strong experimental evidence indicates that the flow of viscoelastic fluids through packed beds can exhibit rapid increases in the pressure drop, or an increase in the apparent viscosity, above that expected for a comparable purely viscous fluid. This increase has been attributed to the extensional nature of the flow field in the pores caused by the successive expansions and contractions that a fluid element experiences as it traverses the pore space. Although the flow field at pore level is not an ideal extensional flow due to the presence of shear and rotation, the increase in flow resistance is referred to as an extension-thickening effect [62, 72, 128, 130–132]. In this regard, two major interrelated aspects have strong impact on the flow through porous media. These are extensional flow and converging-diverging geometry.

### 4.1.1 Extensional Flow

One complexity in the flow in general and through porous media in particular arises from the coexistence of shear and extensional components, sometimes with the added complication of inertia. Pure shear or elongational flow is the exception in practical situations. In most situations mixed flow occurs where deformation rates have components parallel and perpendicular to the principal flow direction. In such flows, the elongational components may be associated with the converging-diverging flow paths [7, 63]. A general consensus has emerged recently that the flow through packed beds has a substantial extensional component and typical polymer solutions exhibit strain hardening in extension, which is one of the main factors for the reported dramatic increases in pressure drop. Thus in principle the shear viscosity alone is inadequate to explain the observed excessive pressure gradients. It is interesting therefore to know the relative importance of elastic and viscous effects or the relationship between normal and shear stresses for different shear rates [9, 47].

An extensional or elongational flow is one in which fluid elements are subjected to extensions and compressions without being rotated or sheared. The study of the extensional flow in general as a relevant variable has only received attention in the last few decades with the realization that extensional flow is of significant relevance in many practical situations. Before that, rheology was largely dominated by shear flow. The historical convention of matching only shear flow data with theoretical predictions in constitutive modeling should be rethought in those areas of interest where there is a large extensional contribution. Extensional flow experiments can be viewed as providing critical tests for any proposed constitutive equations [7, 13, 17, 133].

Extensional flow is fundamentally different from shear flow. The material property characterizing the extensional flow is not the viscosity but the extensional viscosity. The behavior of the extensional viscosity function is often qualitatively different from that of the shear viscosity. For example, highly elastic polymer solutions that possess a viscosity that decreases monotonically in shear often exhibit an extensional viscosity that increases dramatically with extension rate. Thus, while the shear viscosity is shear-thinning, the extensional viscosity is extension-thickening [7, 17]. The extensional or elongational viscosity  $\mu_x$ , also called Trouton viscosity, is defined as the ratio of tensile stress to the extension rate under steady

flow condition where both these quantities attain constant values. Mathematically, it is given by

$$\mu_x = \frac{\tau_E}{\dot{\epsilon}} \quad (20)$$

where  $\tau_E (= \tau_{11} - \tau_{22})$  is the normal stress difference and  $\dot{\epsilon}$  is the extension rate. The stress  $\tau_{11}$  is in the direction of the extension while  $\tau_{22}$  is in a direction perpendicular to the extension [7, 134].

Polymeric fluids show a non-constant extensional viscosity in steady and unsteady extensional flow. In general, extensional viscosity is a function of the extensional strain rate, just as the shear viscosity is a function of shear rate. It is far more difficult to measure the extensional viscosity than the shear viscosity. There is therefore a gulf between the strong desire to measure extensional viscosity and the likely expectation of its fulfilment [7, 18]. A major difficulty that hinders the progress in this field is that it is difficult to achieve steady elongational flow and quantify it precisely. Despite the fact that many techniques have been developed for measuring the elongational flow properties, these techniques failed so far to produce consistent outcome as they generate results which can differ by several orders of magnitude. This indicates that these results are dependent on the method and instrument of measurement. This is highlighted by the view that the extensional viscometers provide measurements of an extensional viscosity rather than the extensional viscosity. The situation is made more complex by the fact that it is almost impossible to generate a pure extensional flow since a shear component is always present in real flow situations, and this makes the measurements doubtful and inconclusive [2, 6, 7, 9, 17, 127].

For Newtonian and inelastic non-Newtonian fluids the extensional viscosity is a constant that only depends on the type of extensional deformation. Moreover, the viscosity measured in a shear flow can be used to predict the viscosity in other types of deformation. For example, in a simple uniaxial extensional flow of a Newtonian fluid the following relationship is satisfied

$$\mu_x = 3\mu_o \quad (21)$$

For viscoelastic fluids the flow behavior is more complex and the extensional viscosity, like the shear viscosity, depends on both the strain rate and the time following the onset of straining. The rheological behavior of a complex fluid in extension is often very different from that in shear. Polymers usually have extremely

high extensional viscosities which can be orders of magnitude higher than those expected on the basis of Newtonian model. Moreover, the extensional viscosities of elastic polymer solutions can be thousands of times greater than their shear viscosities. To measure the departure of the ratio of extensional to shear viscosity from its Newtonian equivalent, the rheologists have introduced what is known as the Trouton ratio which is usually defined as

$$Tr = \frac{\mu_x(\dot{\epsilon})}{\mu_s(\sqrt{3}\dot{\epsilon})} \quad (22)$$

For elastic liquids, the Trouton ratio is expected to be always greater than or equal to 3, with the value 3 only attained at vanishingly small strain rates. These liquids are known for having very high Trouton ratios that can be as high as  $10^4$ . This conduct is expected especially when the fluid combines shear-thinning with tension-thickening. However, even for the fluids that demonstrate tension-thinning the associated Trouton ratios usually increase with strain rate and are still significantly in excess of the inelastic value of three [3, 7, 17, 18, 133, 135].

Figures (10) and (11) compare the shear viscosity to the extensional viscosity at isothermal condition for a typical viscoelastic fluid at various shear and extension rates. As seen in Figure (10), the shear viscosity curve can be divided into three regions. For low-shear rates, compared to the time scale of the fluid, the viscosity is approximately constant. It then equals the so called zero shear rate viscosity. After this initial plateau the viscosity rapidly decreases with increasing shear rate, and this behavior is described as shear-thinning. However, there are some materials for which the reverse behavior is observed, that is the shear viscosity increases with shear rate giving rise to shear-thickening. For high shear rates the viscosity often approximates a constant value again. The constant viscosity extremes at low and high shear rates are known as the lower and upper Newtonian plateau, respectively [6, 7, 18].

In Figure (11) the typical behavior of the extensional viscosity,  $\mu_x$ , of a viscoelastic fluid as a function of extension rate,  $\dot{\epsilon}$ , is depicted. As seen, the extensional viscosity curve can be divided into several regions. At low extension rates the extensional viscosity maintains a constant value known as the zero extension rate extensional viscosity. This is usually three times the zero shear rate viscosity, just as for a Newtonian fluid. For somewhat larger extension rates the exten-

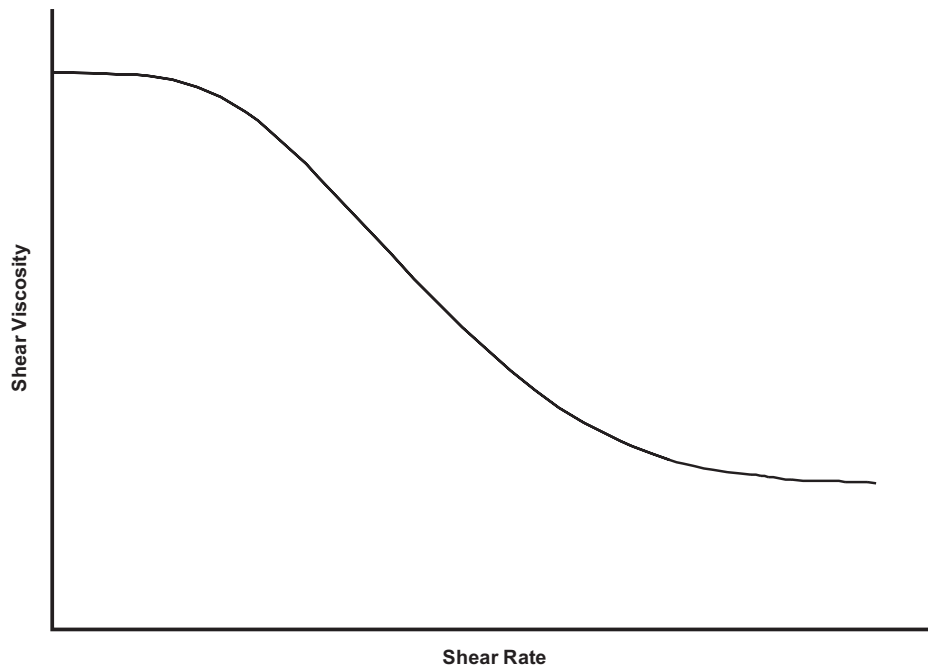


Figure 10: Typical behavior of shear viscosity  $\mu_s$  as a function of shear rate  $\dot{\gamma}$  in shear flow on log-log scales.

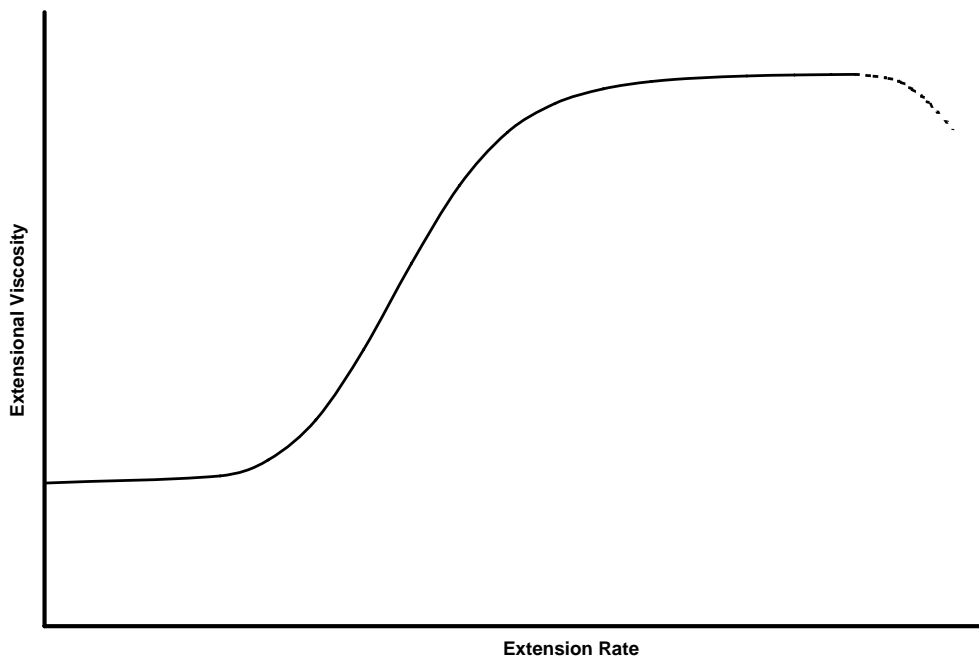


Figure 11: Typical behavior of extensional viscosity  $\mu_x$  as a function of extension rate  $\dot{\epsilon}$  in extensional flow on log-log scales.

sional viscosity increases with increasing extension rate. Some viscoelastic fluids behave differently, that is their extensional viscosity decreases on increasing extension rate in this regime. A fluid for which  $\mu_x$  increases with increasing  $\dot{\epsilon}$  is said to be tension-thickening, whilst if  $\mu_x$  decreases with increasing  $\dot{\epsilon}$  it is described as tension-thinning. For even higher extension rates the extension viscosity reaches a maximum constant value. If the extension rate is increased once more the extensional viscosity may decrease again. It should be remarked that two polymeric liquids that may have essentially the same behavior in shear can show a different response in extension [3, 6, 7, 17].

### 4.1.2 Converging-Diverging Geometry

An important aspect that characterizes the flow in porous media and makes it distinct from bulk is the presence of converging-diverging flow paths. This geometric factor significantly affects the flow and accentuate elastic responses. Several arguments have been presented in the literature to explain the effect of converging-diverging geometry on the flow behavior. One argument is that viscoelastic flow in porous media differs from that of Newtonian flow, primarily because the converging-diverging nature of flow in porous media gives rise to normal stresses which are not solely proportional to the local shear rate. A second argument is that any geometry that involves a diameter change will generate a flow field with elongational characteristics, and hence the flow field in porous media involves both shear and elongational components with elastic responses. A third argument suggests that elastic effects are expected in the flow through porous media because of the acceleration and deceleration of the fluid in the interstices of the bed upon entering and leaving individual pores [54, 55, 68].

Despite this diversity, there is a general consensus that in porous media the converging-diverging nature of the flow paths brings out both the extensional and shear properties of the fluid. The principal mode of deformation to which a material element is subjected as the flow converges into a constriction involves both a shearing of the material element and a stretching or elongation in the direction of flow, while in the diverging portion the flow involves both shearing and compression. The actual channel geometry determines the ratio of shearing to extensional contributions. In many realistic situations involving viscoelastic flows the extensional contribution is the most important of the two modes. As porous media flow involves elongational flow components, the coil-stretch phenomenon can also take

place.

A consequence of the presence of converging-diverging feature in porous media on flow modeling is that a suitable model pore geometry is one having converging and diverging sections which can reproduce the elongational nature of the flow. Despite the general success of the straight capillary tube model with Newtonian and inelastic non-Newtonian flows, its failure with elastic flow is remarkable. To rectify the flaws of this model, the undulating tube and converging-diverging channel were proposed in order to include the elastic character of the flow. Various corrugated tube models with different simple geometries have been used as a first step to model the effect of converging-diverging geometry on the flow of viscoelastic fluids in porous media (e.g. [72, 125, 136]). Those geometries include conically shaped sections, sinusoidal corrugation and abrupt expansions and contractions. Some simplified forms of these geometries are displayed in Figure (9). Similarly, a bundle of converging-diverging tubes forms a better model for a porous medium in viscoelastic flow than the bundle of straight capillary tubes, as the presence of diameter variations makes it possible to account for elongational contributions. Many investigators have attempted to capture the role of successive converging-diverging character of packed bed flow by numerically solving the flow equations in conduits of periodically varying cross sections. Some of these are [13, 47, 62, 68, 137]. Different opinions on the success of these models can be found in the literature. With regards to modeling viscoelastic flow in regular or random networks of converging-diverging capillaries, very little work has been done.

## 4.2 Viscoelastic Effects in Porous Media

In packed bed flows, the main manifestation of steady-state viscoelastic effects is the excess pressure drop or dilatancy behavior in different flow regimes above what is accounted for by shear viscosity of the flowing liquid. Qualitatively, this behavior was attributed either to memory effects or to extensional flow. However, both explanations have a place as long as the flow regime is considered. Furthermore, the geometry of the porous media must be taken into account when considering elastic responses [47, 54].

There is a general agreement that the flow of viscoelastic fluids in packed beds results in a greater pressure drop than what can be ascribed to the shear rate dependent viscosity. Fluids that exhibit elasticity deviate from viscous flow above

some critical velocity in porous flow. At low flow rates, the pressure drop is determined largely by shear viscosity, and the viscosity and elasticity are approximately the same as in bulk. As the flow rate gradually increases, viscoelastic effects begin to appear in various flow regimes. Consequently, the *in situ* rheological characteristics become significantly different from those in bulk as elasticity dramatically increases showing strong dilatant behavior. Although experimental evidence for viscoelastic effects is convincing, an equally convincing theoretical analysis is not available. One general argument is that when the fluid suffers a significant deformation in a time comparable to the relaxation time of the fluid, elastic effects become important [9, 47, 54, 124].

The complexity of viscoelastic flow in porous media is aggravated by the possible occurrence of other non-elastic phenomena which have similar effects as viscoelasticity. These phenomena include adsorption of the polymers on the capillary walls, mechanical retention and partial pore blockage. All these effects also lead to pressure drops well in excess to that expected from the shear viscosity levels. Consequently, the interpretation of many observed effects is controversial. Some authors may interpret some observations in terms of partial pore blockage whereas others insist on non-Newtonian effects including viscoelasticity as an explanation. However, none of these have proved to be completely satisfactory. Moreover, no one can rule out the possibility of simultaneous occurrence of these elastic and inelastic phenomena with further complication and confusion. An interesting fact is the observation made by several researchers, e.g. Sadowski [53], that reproducible results can be obtained only in constant flow rate experiments because at constant pressure drop the velocity kept decreasing. This kind of observation indicates deposition of polymer on the solid surface by one mechanism or another, and cast doubt on some explanations which involve elasticity. At constant flow rate the increased pressure drop seems to provide the necessary force to keep a reproducible portion of the flow channels open [11, 47, 126, 138].

There are three principal viscoelastic effects that have to be accounted for in the investigation of viscoelasticity: transient time-dependence, steady-state time-dependence and dilatancy at high flow rates.

### 4.2.1 Transient Time-Dependence

Transient time-dependent viscoelastic behavior has been observed in bulk on the startup and cessation of processes involving the displacement of viscoelastic materials, and on a sudden change of rate or reversal in the direction of deformation. During these transient states, there are frequently overshoots and undershoots in stress as a function of time which scale with strain. However, if the fluid is strained at a constant rate, these transients die out in the course of time, and the stress approaches a steady-state value that depends only on the strain rate. Under initial flow conditions stresses can reach magnitudes which are substantially more important than their steady-state values, whereas the relaxation on a sudden cessation of strain can vary substantially in various circumstances [6, 9, 17, 24, 29].

Transient responses are usually investigated in the context of bulk rheology, despite the fact that there is no available theory that can predict this behavior quantitatively. As a consequence of this restraint to bulk, the literature of viscoelastic flow in porous media is almost entirely dedicated to the steady-state situation with hardly any work on the *in situ* time-dependent viscoelastic flows. However, transient behavior is expected to occur in similar situations during the flow through porous media. One reason for this gap is the absence of a proper theoretical structure and the experimental difficulties associated with these flows *in situ*. Another possible reason is that the *in situ* transient flows may have less important practical applications.

### 4.2.2 Steady-State Time-Dependence

By this, we mean the effects that arise in the steady-state flow due to time dependency, as time-dependence characteristics of the viscoelastic material must have an impact on the steady-state conduct. Indeed, elastic effects do occur in steady-state flow through porous media because of the time-dependence nature of the flow at pore level. Depending on the time scale of the flow, viscoelastic materials may show viscous or elastic behavior. The particular response in a given process depends on the time scale of the process in relation to a natural time of the material. With regard to this time scale dependency of viscoelastic flow process at pore level, the fluid relaxation time and the rate of elongation or contraction that occurs as the fluid flows through a channel or pore with varying cross sectional area should be used to characterize and quantify viscoelastic behavior [7, 54, 125, 139].

Sadowski and Bird [10] analyzed the viscometric flow problem in a long straight circular tube and argued that in such a flow no time-dependent elastic effects are expected. However, in a porous medium elastic effects may occur. As the fluid moves through a tortuous channel in the porous medium, it encounters a capriciously changing cross-section. If the fluid relaxation time is small with respect to the transit time through a contraction or expansion in a tortuous channel, the fluid will readjust to the changing flow conditions and no elastic effects would be observed. If, on the other hand, the fluid relaxation time is large with respect to the time to go through a contraction or expansion, then the fluid will not accommodate and elastic effects will be observed in the form of an extra pressure drop or an increase in the apparent viscosity. Thus the concept of a ratio of characteristic times emerges as an ordering parameter in viscoelastic flow through porous media. This indicates the importance of the ratio of the natural time of a fluid to the duration time of a process [11]. It is noteworthy that this formulation relies on a twofold ordering scheme and is valid for some systems and flow regimes. More elaborate formulation will be given in conjunction with the intermediate plateau phenomenon.

One of the steady-state viscoelastic phenomena observed in the flow through porous media and can be qualified as a time-dependent effect, among other possibilities such as retention, is the intermediate plateau at medium flow rates as demonstrated in Figure (3). A possible explanation is that at low flow rates before the appearance of the intermediate plateau the fluid behaves inelastically like any typical shear-thinning fluid. This implies that in the low flow regime viscoelastic effects are negligible as the fluid can respond to the local state of deformation almost instantly, that is it does not remember its past and hence behaves as a purely viscous fluid. As the flow rate increases, a point will be reached where the solid-like characteristics of viscoelastic materials begin to appear in the form of an increased apparent viscosity as the time of process becomes comparable to the natural time of fluid, and hence a plateau is observed. At higher flow rates the process time is short compared to the natural time of the fluid and hence the fluid has no time to react as the fluid is not an ideal elastic solid that reacts instantaneously. Since the process time is very short, no overshoot will occur at the tube constriction as a measurable finite time is needed for the overshoot to take place. The result is that no increase in the pressure drop will be observed in this flow regime and the normal shear-thinning behavior is resumed with the eventual high flow rate plateau [125, 140].

It is noteworthy that Dauben and Menzie [126] have discussed a similar issue in conjunction with the effect of diverging-converging geometry on the flow through porous media. They argued that the process of expansion and contraction repeated many times may account in part for the high pressure drops encountered during viscoelastic flow in porous media. The fluid relaxation time combined with the flow velocity determines the response of the viscoelastic fluid in the suggested diverging-converging model. Accordingly, it is possible that if the relaxation time is long enough or the fluid velocity high enough the fluid can pass through the large opening before it has had time to respond to a stress change imposed at the opening entrance, and hence the fluid would behave more as a viscous and less like a viscoelastic.

### 4.2.3 Dilatancy at High Flow Rates

The third distinctive feature of viscoelastic flow is the dilatant behavior in the form of excess pressure losses at high flow rates as depicted in Figure (4). Certain polymeric solutions that exhibit shear-thinning in a viscometric flow seem to exhibit a shear-thickening response under appropriate conditions during flow through porous media. At high flow rates, abnormal increases in flow resistance that resemble a shear-thickening response have been observed in flow experiments involving a variety of dilute to moderately concentrated solutions of high molecular weight polymers [11, 63]. This phenomenon can be attributed to stretch-thickening due to the dominance of extensional over shear flow. At high flow rates, strong extensional flow effects do occur and the extensional viscosity rises very steeply with increasing extension rate. As a result, the non-shear terms become much larger than the shear terms. For Newtonian fluids, the extensional viscosity is just three times the shear viscosity. However, for viscoelastic fluids the shear and extensional viscosities often behave oppositely, that is while the shear viscosity is generally a decreasing function of the shear rate, the extensional viscosity increases as the extension rate increases. The consequence is that the pressure drop will be governed by extension-thickening and the apparent viscosity rises sharply. Other possibilities such as physical retention are less likely to take place at these high flow rates [40, 127].

Finally, a glimpse on the literature of viscoelastic flow in porous media will help to clarify the situation and highlight some important contributions in this

field. Sadowski and Bird [10, 52, 53] were the first to include elastic effects in their rheological model to account for a departure of the experimental data in porous media from the modified Darcy's law [11, 63]. Wissler [124] was the first to account quantitatively for the elongational stresses developed in viscoelastic flow through porous media [68]. In this context, he presented a third order perturbation analysis of a viscoelastic fluid flow through a converging-diverging channel. Gogarty *et al* [54] developed a modified form of the non-Newtonian Darcy equation to predict the viscous and elastic pressure drop versus flow rate relationships for the flow of elastic carboxymethylcellulose (CMC) solutions in beds of different geometries. Park *et al* [55] studied the flow of various polymeric solutions through packed beds using several rheological models. In the case of one type of solution at high Reynolds numbers they introduced an empirical corrections based upon a pseudo viscoelastic Deborah number to improve the data fit.

In their investigation to the flow of polymers through porous media, Hirasaki and Pope [139] modeled the dilatant behavior by viscoelastic properties of the polymer solution. The additional viscoelastic resistance to the flow, which is a function of Deborah number, was modeled as a simple elongational flow to represent the elongation and contraction that occur as the fluid flows through a pore with varying cross sectional area. Deiber and Schowalter [13, 72] used a circular tube with a radius which varies sinusoidally in the axial direction as a first step toward modeling the flow channels of a porous medium. They concluded that such a tube exhibits similar phenomenological aspects to those found for the flow of viscoelastic fluids through packed beds. Durst *et al* [40] highlighted the fact that the pressure drop of a porous medium flow is only due to a small extent to the shear force term usually employed to derive the Kozeny-Darcy law. For a more correct derivation, additional terms have to be taken into account since the fluid is also exposed to elongational forces when it passes through the porous media matrix. Chmielewski and coworkers [141–143] investigated the elastic behavior of polyisobutylene solutions flowing through arrays of cylinders with various geometries. They recognized that the converging-diverging geometry of the pores in porous media causes an extensional flow component that may be associated with the increased flow resistance for viscoelastic liquids. Pilitsis *et al* [73] simulated the flow of a shear-thinning viscoelastic fluid through a periodically constricted tube using a variety of constitutive rheological models, and the results were compared against the experimental data of Deiber and Schowalter [72]. It was found that the presence of the elasticity in the mathematical model caused an increase

in the flow resistance over the value calculated for the viscous fluid. Talwar and Khomami [68] developed a higher order Galerkin finite element scheme for simulating two-dimensional viscoelastic flow and successfully tested the algorithm with the flow of Upper Convected Maxwell (UCM) and Oldroyd-B fluids in undulating tube. It was subsequently used to solve the problem of transverse steady flow of UCM and Oldroyd-B fluids past an infinite square arrangement of infinitely long, rigid, motionless cylinders.

Garrouch [144] developed a generalized viscoelastic model for polymer flow in porous media analogous to Darcy's law, and hence concluded a nonlinear relationship between the fluid velocity and pressure gradient. The model accounts for polymer elasticity by using the longest relaxation time, and accounts for polymer viscous properties by using an average porous medium power-law behavior index. Koshiha *et al* [145] investigated the viscoelastic flow through an undulating channel as a model for flow paths in porous media and concluded that the stress in the flow through the undulating channel should rapidly increase with increasing flow rate because of the stretch-thickening elongational viscosity. Khuzhayorov *et al* [146] applied a homogenization technique to derive a macroscopic filtration law for describing transient linear viscoelastic fluid flow in porous media. The results obtained in the particular case of the flow of an Oldroyd fluid in a bundle of capillary tubes show that viscoelastic behavior strongly differs from Newtonian behavior. Huifen *et al* [147] developed a model for the variation of rheological parameters along the seepage flow direction and constructed a constitutive equation for viscoelastic fluids in which the variation of the rheological parameters of polymer solutions in porous media is taken into account. Mendes and Naccache [127] employed a simple theoretical approach to obtain a constitutive relation for the flows of extension-thickening fluids through porous media. The pore morphology is assumed to be composed of a bundle of periodically converging-diverging tubes. Dolejš *et al* [148] presented a method for the pressure drop calculation for the flow of viscoelastic fluids through fixed beds of particles. The method is based on the application of the modified Rabinowitsch-Mooney equation together with the corresponding relations for consistency variables.

## 5 Thixotropy and Rheopexy

Time-dependent fluids are defined to be those fluids whose viscosity depends on the duration of flow under isothermal conditions. For these fluids, a time-independent steady-state viscosity is eventually reached in steady flow situation. The time effect is often reversible though it may be partial, that is the trend of the viscosity change is overturned in time when the stress is reduced. The phenomenon is generally attributed to time-dependent thixotropic breakdown or rheopectic buildup of some particulate structure under relatively high stress followed by structural change in the opposite direction for lower stress, though the exact mechanism may not be certain [8, 9, 34, 149, 150].

Time-dependent fluids are generally divided into two main categories: thixotropic (work softening) whose viscosity gradually decreases with time at a constant shear rate, and rheopectic (work hardening or anti-thixotropic or negative thixotropic) whose viscosity increases under similar circumstances without an overshoot which is a characteristic feature of viscoelasticity. However, it has been proposed that rheopexy and negative thixotropy are different, and hence three categories of time-dependent fluids do exist [3, 9, 151]. It is noteworthy that in this article we may rely on the context and use ‘thixotropy’ conveniently to indicate non-elastic time-dependence in general where the meaning is obvious.

Thixotropic fluids may be described as shear-thinning while the rheopectic as shear-thickening, in the sense that these effects take place on shearing, though they are effects of time-dependence. However, it is proposed that thixotropy invariably occurs in circumstances where the liquid is shear-thinning (in the usual sense of viscosity decrease with increasing shear rate) while rheopexy may be associated with shear-thickening. This can be behind the occasional confusion between thixotropy and shear-thinning [7, 27, 34, 152].

A substantial number of complex fluids display time-dependence phenomena, with thixotropy being more commonplace and better understood than rheopexy. Various mathematical models have been proposed to describe time-dependence behavior. These include microstructural, continuum mechanics, and structural kinetics models. Thixotropic and rheopectic behaviors may be detected by the hysteresis loop test, as well as by the more direct steady shear test. In the loop test the substance is sheared cyclically and a graph of stress versus shear rate

is obtained. A time-dependent fluid should display a hysteresis loop the area of which is a measure of the degree of thixotropy or rheopexy and this may be used to quantify time-dependent behavior [2, 8, 150–152].

In theory, time-dependence effects can arise from thixotropic structural change or from viscoelasticity. The existence of these two different types of time-dependent rheologies is generally recognized. Although it is convenient to distinguish between these as separate types of phenomena, real fluids can exhibit both types of rheology at the same time. Several physical distinctions between viscoelastic and thixotropic time-dependence have been made. The important one is that while the time-dependence of viscoelastic fluids arises because the response of stresses and strains in the fluid to changes in imposed strains and stresses respectively is not instantaneous, in thixotropic fluids such response is instantaneous and the time-dependent behavior arises purely because of changes in the structure of the fluid as a consequence of strain. While the mathematical theory of viscoelasticity has been developed to an advanced level, especially on the continuum mechanical front, relatively little work has been done on thixotropy and rheopexy. One reason is the lack of a comprehensive framework to describe the dynamics of thixotropy. This may partly explain why thixotropy is rarely incorporated in the constitutive equation when modeling the flow of non-Newtonian fluids. The underlying assumption is that in these situations the thixotropic effects have a negligible impact on the resulting flow field, and this allows great mathematical simplifications [51, 149, 151, 153–155].

Several behavioral distinctions can be made to differentiate between viscoelasticity and thixotropy. These include the presence or absence of some characteristic elastic features such as recoil and normal stresses. However, these signs may be of limited use in some practical situations involving complex fluids where these two phenomena coexist. In Figure (12) the behavior of these two types of fluids in response to step change in strain rate is compared. Although both fluids show signs of dependency on the past history, the graph suggests that inelastic thixotropic fluids do not possess a memory in the same sense as viscoelastic materials. The behavioral differences, such as the absence of elastic effects or the difference in the characteristic time scale associated with these phenomena, confirm this suggestion [9, 34, 152, 153].

Thixotropy, like viscoelasticity, is a phenomenon that can appear in a large

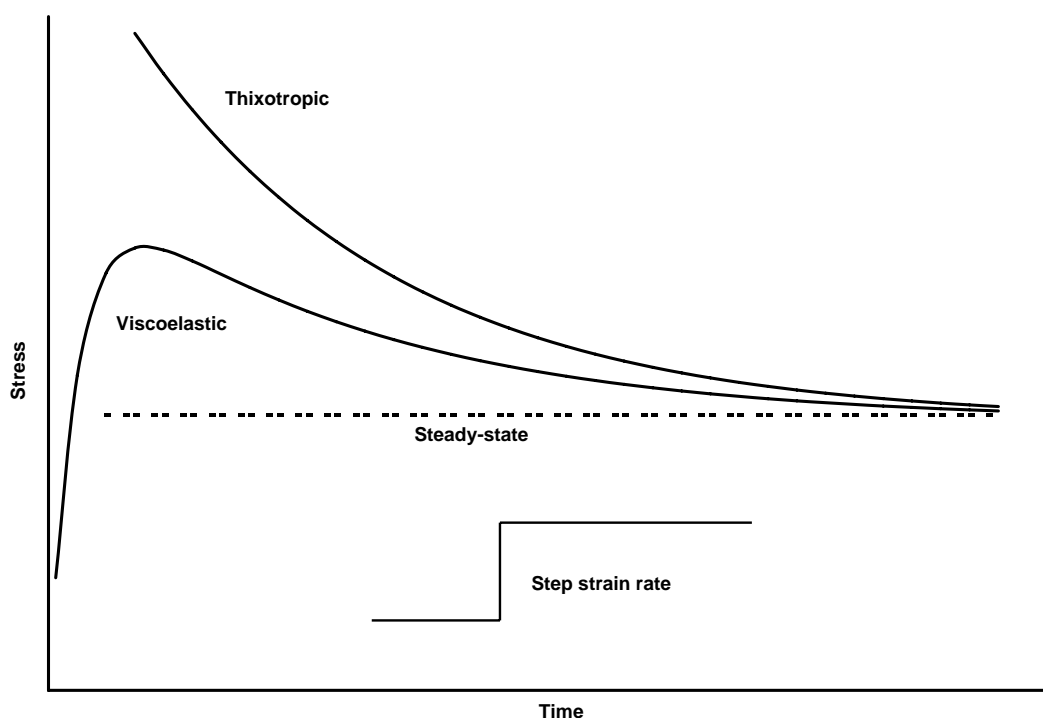


Figure 12: Comparison between time dependency in thixotropic and viscoelastic fluids following a step increase in strain rate.

number of systems. The time scale for thixotropic changes is measurable in various materials including important commercial and biological products. However, the investigation of thixotropy has been hampered by several difficulties. Consequently, the suggested thixotropic models seem unable to present successful quantitative description of thixotropic behavior especially for the transient state. In fact, even the most characteristic property of thixotropic fluids, i.e. the decay of viscosity or stress under steady shear conditions, presents difficulties in modeling and characterization. The lack of a comprehensive theoretical framework to describe thixotropy is matched by a severe shortage on the experimental side. One reason is the difficulties confronted in measuring thixotropic systems with sufficient accuracy. As a result, very few systematic data sets can be found in the literature and this deficit hinders the progress in this field. Moreover, the characterization of the data in the absence of an agreed-upon mathematical structure may be questionable [33, 149, 150, 152, 153].

## 5.1 Modeling Time-Dependent Flow in Porous Media

In the absence of serious attempts to model thixotropic rheology in porous media using the four major modeling approaches (i.e. continuum, capillary bundle, numerical methods and network modeling), very little can be said about this issue. It seems, however, that network modeling is currently the best candidate for dealing with this task. In this context, There are three major cases of simulating the flow of time-dependent fluids in porous media

- The flow of strongly strain-dependent fluid in a porous medium that is not very homogeneous. This case is very difficult to model because of the difficulty to track the fluid elements in the pores and throats and determine their deformation history. Moreover, the viscosity function is not well defined due to the mixing of fluid elements with various deformation history in the individual pores and throats.
- The flow of strain-independent or weakly strain-dependent fluid through porous media in general. A possible strategy is to apply single time-dependent viscosity function to all pores and throats at each instant of time and hence simulating time development as a sequence of Newtonian states.
- The flow of strongly strain-dependent fluid in a very homogeneous porous medium such that the fluid is subject to the same deformation in all network elements. The strategy for modeling this flow is to define an effective pore strain rate. Then using a very small time step the strain rate in the next instant of time can be found assuming constant strain rate. As the change in the strain rate is now known, a correction to the viscosity due to strain-dependency can be introduced.

There are two possible problems in this strategy. The first is edge effects in the case of injection from a reservoir because the deformation history of the fluid elements at the inlet is different from the deformation history of the fluid elements inside the network. The second is that considerable computing resources may be required if very small time steps are used.

The flow of time-dependent fluids in porous media has not been vigorously investigated. Consequently, very few studies can be found in the literature on this subject. One reason is that time-dependent effects are usually investigated in the

context of viscoelasticity. Another reason is the lack of a comprehensive framework to describe the dynamics of time-dependent fluids in porous media [51, 151, 155]. Among the few examples that we found on this subject is the investigation of Pritchard and Pearson [155] of viscous fingering instability during the injection of a thixotropic fluid into a porous medium or a narrow fracture. Another example is the study by Wang *et al* [156] who examined thixotropic effects in the context of heavy oil flow through porous media. Finally, some thixotropic aspects were modeled by Sochi [77, 129] using network modeling approach as part of implementing the Bautista-Manero rheological model which incorporates thixotropic as well as viscoelastic effects.

## 6 Experimental Work on Non-Newtonian Flow in Porous Media

For completion, we include a brief non-comprehensive list of some experimental work in the field of non-Newtonian flow through porous media. This collection should provide a feeling of the nature and topics of experimental research in the last few decades. The list is arranged in a chronological order

- Sadowski [52, 53] conducted extensive experimental work on the flow of polymeric solutions through packed beds. He used ten aqueous polymeric solutions made from Carbowax 20-M, Elvanol 72-51, Natrosol 250G and Natrosol 250H with various concentrations. The porous media were packed beds of lead shot or glass beads with different properties. He used Ellis as a rheological model for the fluids and introduced a characteristic time to designate regions of behavior where elastic effects are important.
- Marshall and Metzner [125] used three polymeric non-Newtonian solutions (Carbopol 934, polyisobutylene L100 and ET-597) to investigate the flow of viscoelastic fluids through porous media and determine a Deborah number at which viscoelastic effects first become measurable. The porous medium which they used was a sintered bronze porous disk.
- White [157] conducted simple experiments on the flow of a hydroxyethylcellulose solution through a stratified bed using a power-law form of Darcy's Law.
- Gogarty *et al* [54] carried out experiments on the flow of polymer solutions of carboxymethylcellulose (CMC) and polyacrylamide through three packed beds of glass beads with various size and a packed bed of sand.
- Park *et al* [55, 56] experimentally studied the flow of polymeric aqueous solutions of polymethylcellulose (PMC) with different molecular weights and concentrations through two packed beds of spherical uniform-in-size glass beads, coarse and fine. Several rheological models, including Ellis and Herschel-Bulkley, were used to characterize the fluids.
- Teeuw and Hesselink [158] carried out core flow experiments to investigate the behavior of aqueous biopolymer solutions in porous media. They used

cylindrical plugs of Bentheim, a clean outcrop sandstone of very uniform grain size and structure, as porous media characterizing the solutions with power-law.

- Vogel and Pusch [159] conducted flow experiments on sand pack using three polymeric solutions: a polysaccharide, a hydroxyethylcellulose and a polyacrylamide.
- Al-Fariss and Pinder [58] conducted experimental work on waxy oils modeled as Herschel-Bulkley fluids. The porous media consist of two packed beds of sand having different dimensions, porosity, permeability and grain size.
- Durst *et al* [40] verified aspects of their theoretical non-Newtonian investigation by experimental work on the flow of dilute polymer solutions through porous media of packed spheres.
- Sorbie *et al* [160] conducted an extensive experimental and theoretical investigation on the single-phase flow of Xanthan/tracer slugs in a consolidated sandstone using Carreau rheology. The phenomena studied include polymer/tracer dispersion, excluded volume effects, polymer adsorption, and viscous fingering.
- Cannella *et al* [61] experimentally investigated the flow of Xanthan solutions through Berea sandstone and carbonate cores in the presence and absence of residual oil. They used modified power-law and Carreau rheologies in their theoretical analysis.
- Chmielewski *et al* [141–143] conducted experiments to investigate the elastic behavior of the flow of polyisobutylene solutions through arrays of cylinders with various geometries.
- Chhabra and Srinivas [161] conducted experimental work investigating the flow of power-law liquids through beds of non-spherical particles using the Ergun equation to correlate the resulting values of friction factor. They used beds of three different types of packing materials (two sizes of Raschig rings and one size of gravel chips) as porous media and solutions of carboxymethylcellulose as shear-thinning liquids.
- Fletcher *et al* [162] investigated the flow of biopolymer solutions of Flocon 4800MXC, Xanthan CH-100-23, and scleroglucan through Berea and

Clashach cores utilizing Carreau rheological model to characterize the fluids.

- Hejri *et al* [163] investigated the rheological behavior of biopolymer solutions of Flocon 4800MX characterized by power-law in sand pack cores.
- Sabiri and Comiti [164] investigated the flow of non-Newtonian purely viscous fluids through packed beds of spherical particles, long cylinders and very flat plates. They used aqueous polymeric solutions of carboximethylcellulose sodium salt. The rheological behavior of these solutions was represented by a series of power-law type equations.
- Saunders *et al* [165] carried experimental studies on viscoelastic compression of resin-impregnated fibre cloths. The experiments included a type of plain-weave cloth and two types of resin, an epoxy behaving approximately as a Newtonian fluid and a polyester following power-law non-Newtonian behavior.
- Chase and Dachavijit [60] performed experimental research on aqueous solutions of Carbopol 941 with various concentrations modeled as Bingham fluids. The porous medium was a packed column of spherical glass beads having a narrow size distribution.
- Kuzhir *et al* [166] investigated the flow of a Bingham magneto-rheological (MR) fluid through different types of porous medium which include bundles of cylinders and beds of magnetic and non-magnetic spheres.
- D'Angelo *et al* [167] used radioactive techniques to study the dispersion and retention phenomena of non-Newtonian scleroglucan polymeric solutions in a porous medium consisting of an acrylic cylinder filled with compacted glass microspheres.
- Balhoff and Thompson [97, 98] carried out a limited amount of experimental work (single dataset) on the flow of guar gum solution in a packed bed of glass beads. Ellis rheology was used to characterize the fluid.
- Perrin *et al* [99] conducted experimental work on the flow of hydrolyzed polyacrylamide (HPAM) solutions in two-dimensional etched silicon wafer micromodels as idealizations of porous media. The results from these experiments were analyzed by pore-scale network modeling incorporating the non-Newtonian fluid mechanics of a Carreau fluid.

- Wang *et al* [156] carried out experimental work on dead oils obtained from four wells in the Chinese Zaoyuan oilfield by injecting oil into sand pack cores. The investigation included yield-stress, viscoelastic and thixotropic aspects using Herschel-Bulkley model.
- Schevena *et al* [168] conducted experimental research on Newtonian and non-Newtonian flows through rocks and bead packs. The experiments involved the use of shear-thinning Xanthan solutions and packed beds of near-monodisperse Ballotini beads.

## 7 Conclusions

In the context of fluid flow, ‘non-Newtonian’ is a generic term that incorporates a variety of phenomena. These phenomena are highly complex and require sophisticated mathematical modeling techniques for proper description. Further complications are added when considering the flow through porous media. So far no general methodology that can deal with all cases of non-Newtonian flow has been developed. Moreover, only modest success has been achieved by any one of these methodologies. This situation is not expected to change substantially in the foreseeable future, and many challenges are still waiting to overcome. In the absence of a general approach that is suitable for all situations, a combination of all available approaches is required to tackle non-Newtonian challenges.

Currently, network modeling is the most realistic choice for modeling non-Newtonian flow in porous media. While this approach is capable of predicting the general trend in many situations, it is still unable to account for all complexities and make precise predictions in all cases. The way forward is to improve the modeling strategies and techniques. One requirement is the improvement of pore space definition. While modeling the converging-diverging feature of the pore space with idealized geometry is a step forward, it is not enough. This feature is only one factor in the making of the complex structure of flow channels. The actual geometry and topology in porous media is much more complex and should be fully considered for successful modeling of flow field. Including more physics in the flow description at pore level is another requirement for reaching the final objective.

## 8 Appendix A

### Terminology of Flow and Viscoelasticity\*

A tensor is an array of numbers which transform according to certain rules under coordinate change. In a three-dimensional space, a tensor of order  $n$  has  $3^n$  components which may be specified with reference to a given coordinate system. Accordingly, a scalar is a zero-order tensor and a vector is a first-order tensor.

A stress is defined as a force per unit area. Because both force and area are vectors, considering the orientation of the normal to the area, stress has two directions associated with it instead of one as with vectors. This indicates that stress should be represented by a second-order tensor, given in Cartesian coordinate system by

$$\boldsymbol{\tau} = \begin{pmatrix} \tau_{xx} & \tau_{xy} & \tau_{xz} \\ \tau_{yx} & \tau_{yy} & \tau_{yz} \\ \tau_{zx} & \tau_{zy} & \tau_{zz} \end{pmatrix} \quad (23)$$

where  $\tau_{ij}$  is the stress in the  $j$ -direction on a surface normal to the  $i$ -axis. A shear stress is a force that a flowing liquid exerts on a surface, per unit area of that surface, in the direction parallel to the flow. A normal stress is a force per unit area acting normal or perpendicular to a surface. The components with identical subscripts represent normal stresses while the others represent shear stresses. Thus  $\tau_{xx}$  is a normal stress acting in the  $x$ -direction on a face normal to  $x$ -direction, while  $\tau_{yx}$  is a shear stress acting in the  $x$ -direction on a surface normal to the  $y$ -direction, positive when material at greater  $y$  exerts a shear in the positive  $x$ -direction on material at lesser  $y$ . Normal stresses are conventionally positive when tensile. The stress tensor is symmetric that is  $\tau_{ij} = \tau_{ji}$  where  $i$  and  $j$  represent  $x$ ,  $y$  or  $z$ . This symmetry is required by angular momentum considerations to satisfy equilibrium of moments about the three axes of any fluid element. This means that the state of stress at a point is determined by six, rather than nine, independent stress components.

Viscoelastic fluids show normal stress differences in steady shear flows. The

---

\*In preparing this Appendix, we consulted most of our references. The main ones are [1, 4, 6, 7, 17, 18, 24, 169, 170].

first normal stress difference  $N_1$  is defined as

$$N_1 = \tau_{11} - \tau_{22} \quad (24)$$

where  $\tau_{11}$  is the normal stress component acting in the direction of flow and  $\tau_{22}$  is the normal stress in the gradient direction. The second normal stress difference  $N_2$  is defined as

$$N_2 = \tau_{22} - \tau_{33} \quad (25)$$

where  $\tau_{33}$  is the normal stress component in the indifferent direction. The magnitude of  $N_2$  is in general much smaller than  $N_1$ . For some viscoelastic fluids,  $N_2$  may be virtually zero. Often not the first normal stress difference  $N_1$  is given, but a related quantity: the first normal stress coefficient. This coefficient is defined by  $\Psi_1 = \frac{N_1}{\dot{\gamma}^2}$  and decreases with increasing shear rate. Different conventions about the sign of the normal stress differences do exist. However, in general  $N_1$  and  $N_2$  show opposite signs. Viscoelastic solutions with almost the same viscosities may have very different values of normal stress differences. The presence of normal stress differences is a strong indication of viscoelasticity, though some associate these properties with non-viscoelastic fluids.

The total stress tensor, also called Cauchy stress tensor, is usually divided into two parts: hydrostatic stress tensor and extra stress tensor. The former represents the hydrostatic pressure while the latter represents the shear and extensional stresses caused by the flow. In equilibrium the pressure reduces to the hydrostatic pressure and the extra stress tensor  $\boldsymbol{\tau}$  vanishes. The extra stress tensor is determined by the deformation history and has to be specified by the constitutive equation of the particular fluid.

The rate of strain or rate of deformation tensor is a symmetric second order tensor which gives the components, both extensional and shear, of the strain rate. In Cartesian coordinate system it is given by:

$$\dot{\boldsymbol{\gamma}} = \begin{pmatrix} \dot{\gamma}_{xx} & \dot{\gamma}_{xy} & \dot{\gamma}_{xz} \\ \dot{\gamma}_{yx} & \dot{\gamma}_{yy} & \dot{\gamma}_{yz} \\ \dot{\gamma}_{zx} & \dot{\gamma}_{zy} & \dot{\gamma}_{zz} \end{pmatrix} \quad (26)$$

where  $\dot{\gamma}_{xx}$ ,  $\dot{\gamma}_{yy}$  and  $\dot{\gamma}_{zz}$  are the extensional components while the others are the

shear components. These components are given by:

$$\begin{aligned}\dot{\gamma}_{xx} &= 2\frac{\partial v_x}{\partial x} & \dot{\gamma}_{yy} &= 2\frac{\partial v_y}{\partial y} & \dot{\gamma}_{zz} &= 2\frac{\partial v_z}{\partial z} \\ \dot{\gamma}_{xy} &= \dot{\gamma}_{yx} & &= \frac{\partial v_x}{\partial y} + \frac{\partial v_y}{\partial x} \\ \dot{\gamma}_{yz} &= \dot{\gamma}_{zy} & &= \frac{\partial v_y}{\partial z} + \frac{\partial v_z}{\partial y} \\ \dot{\gamma}_{xz} &= \dot{\gamma}_{zx} & &= \frac{\partial v_x}{\partial z} + \frac{\partial v_z}{\partial x}\end{aligned}\quad (27)$$

where  $v_x$ ,  $v_y$  and  $v_z$  are the velocity components in the respective directions  $x$ ,  $y$  and  $z$ .

The stress tensor is related to the rate of strain tensor by the constitutive or rheological equation of the fluid which takes a differential or integral form. The rate of strain tensor  $\dot{\boldsymbol{\gamma}}$  is related to the fluid velocity vector  $\mathbf{v}$ , which describes the steepness of velocity variation as one moves from point to point in any direction in the flow at a given instant in time, by the relation

$$\dot{\boldsymbol{\gamma}} = \nabla \mathbf{v} + (\nabla \mathbf{v})^T \quad (28)$$

where  $(.)^T$  is the tensor transpose and  $\nabla \mathbf{v}$  is the fluid velocity gradient tensor defined by

$$\nabla \mathbf{v} = \begin{pmatrix} \frac{\partial v_x}{\partial x} & \frac{\partial v_x}{\partial y} & \frac{\partial v_x}{\partial z} \\ \frac{\partial v_y}{\partial x} & \frac{\partial v_y}{\partial y} & \frac{\partial v_y}{\partial z} \\ \frac{\partial v_z}{\partial x} & \frac{\partial v_z}{\partial y} & \frac{\partial v_z}{\partial z} \end{pmatrix} \quad (29)$$

with  $\mathbf{v} = (v_x, v_y, v_z)$ . It should be remarked that the sign and index conventions used in the definitions of these tensors are not universal.

A fluid possesses viscoelasticity if it is capable of storing elastic energy. A sign of this is that stresses within the fluid persist after the deformation has ceased. The duration of time over which appreciable stresses persist after cessation of deformation gives an estimate of what is called the relaxation time. The relaxation and retardation times,  $\lambda_1$  and  $\lambda_2$  respectively, are important physical properties of viscoelastic fluids because they characterize whether viscoelasticity is likely to be important within an experimental or observational timescale. They usually have the physical significance that if the motion is suddenly stopped the stress decays as  $e^{-t/\lambda_1}$ , and if the stress is removed the rate of strain decays as  $e^{-t/\lambda_2}$ .

For viscous flow, the Reynolds number  $Re$  is a dimensionless number defined as the ratio of the inertial to viscous forces and is given by

$$Re = \frac{\rho l_c v_c}{\mu} \quad (30)$$

where  $\rho$  is the mass density of the fluid,  $l_c$  is a characteristic length of the flow system,  $v_c$  is a characteristic speed of the flow and  $\mu$  is the viscosity of the fluid.

For viscoelastic fluids the key dimensionless group is the Deborah number which is a measure of elasticity. This number may be interpreted as the ratio of the magnitude of the elastic forces to that of the viscous forces. It is defined as the ratio of a characteristic time of the fluid  $\lambda_c$  to a characteristic time of the flow system  $t_c$

$$De = \frac{\lambda_c}{t_c} \quad (31)$$

The Deborah number is zero for a Newtonian fluid and is infinite for a Hookean elastic solid. High Deborah numbers correspond to elastic behavior and low Deborah numbers to viscous behavior. As the characteristic times are process-dependent, materials may not have a single Deborah number associated with them.

Another dimensionless number which measures the elasticity of the fluid is the Weissenberg number  $We$ . It is defined as the product of a characteristic time of the fluid  $\lambda_c$  and a characteristic strain rate  $\dot{\gamma}_c$  in the flow

$$We = \lambda_c \dot{\gamma}_c \quad (32)$$

Other definitions to Deborah and Weissenberg numbers are also in common use and some even do not differentiate between the two numbers. The characteristic time of the fluid may be taken as the largest time constant describing the molecular motions, or a time constant in a constitutive equation. The characteristic time for the flow can be the time interval during which a typical fluid element experiences a significant sequence of kinematic events or it is taken to be the duration of an experiment or experimental observation. Many variations in defining and quantifying these characteristics do exist, and this makes Deborah and Weissenberg numbers not very well defined and measured properties and hence the interpretation of the experiments in this context may not be totally objective.

The Boger fluids are constant-viscosity non-Newtonian elastic fluids. They

played important role in the recent development of the theory of fluid elasticity as they allow dissociation between elastic and viscous effects. Boger realized that the complication of variable viscosity effects can be avoided by employing test liquids which consist of low concentrations of flexible high molecular weight polymers in very viscous solvents, and these solutions are nowadays called Boger fluids.

## 9 Appendix B

### Nomenclature

$\alpha$	parameter in Ellis model
$\gamma$	strain
$\dot{\gamma}$	rate of strain ( $\text{s}^{-1}$ )
$\dot{\gamma}_c$	characteristic rate of strain ( $\text{s}^{-1}$ )
$\dot{\boldsymbol{\gamma}}$	rate of strain tensor
$\epsilon$	porosity
$\varepsilon$	extension
$\dot{\varepsilon}$	rate of extension ( $\text{s}^{-1}$ )
$\lambda$	structural relaxation time in Fredrickson model (s)
$\lambda_1$	relaxation time (s)
$\lambda_2$	retardation time (s)
$\lambda_c$	characteristic time of fluid (s)
$\lambda'$	first time constant in Godfrey model (s)
$\lambda''$	second time constant in Godfrey model (s)
$\lambda_s$	time constant in Stretched Exponential Model (s)
$\mu$	viscosity (Pa.s)
$\mu_e$	effective viscosity (Pa.s)
$\mu_i$	initial-time viscosity (Pa.s)
$\mu_{inf}$	infinite-time viscosity (Pa.s)
$\mu_o$	zero-shear viscosity (Pa.s)
$\mu_s$	shear viscosity (Pa.s)
$\mu_x$	extensional (elongational) viscosity (Pa.s)
$\mu_\infty$	infinite-shear viscosity (Pa.s)
$\Delta\mu'$	viscosity deficit associated with $\lambda'$ in Godfrey model (Pa.s)
$\Delta\mu''$	viscosity deficit associated with $\lambda''$ in Godfrey model (Pa.s)
$\rho$	fluid mass density ( $\text{kg.m}^{-3}$ )
$\tau$	stress (Pa)
$\boldsymbol{\tau}$	stress tensor
$\tau_{1/2}$	stress when $\mu = \mu_o/2$ in Ellis model (Pa)

$\tau_o$	yield-stress (Pa)
$c$	dimensionless constant in Stretched Exponential Model
$C$	consistency factor in power-law and Herschel-Bulkley models (Pa.s <sup><i>n</i></sup> )
$C'$	tortuosity factor
$De$	Deborah number
$D_p$	particle diameter (m)
$G$	geometric conductance (m <sup>4</sup> )
$G'$	flow conductance (m <sup>3</sup> .Pa <sup>-1</sup> .s <sup>-1</sup> )
$G_o$	elastic modulus (Pa)
$k$	parameter in Fredrickson model (Pa <sup>-1</sup> )
$K$	absolute permeability (m <sup>2</sup> )
$L$	length of tube or bed (m)
$l_c$	characteristic length of the flow system (m)
$n$	flow behavior index
$N_1$	first normal stress difference (Pa)
$N_2$	second normal stress difference (Pa)
$P$	pressure (Pa)
$\Delta P$	pressure drop (Pa)
$q$	superficial (Darcy) velocity (m.s <sup>-1</sup> )
$Q$	volumetric flow rate (m <sup>3</sup> .s <sup>-1</sup> )
$R$	tube radius (m)
$Re$	Reynolds number
$R_{eq}$	equivalent radius (m)
$t$	time (s)
$t_c$	characteristic time of flow system (s)
$Tr$	Trouton ratio
$\mathbf{v}$	fluid velocity vector
$\nabla \mathbf{v}$	fluid velocity gradient tensor
$v_c$	characteristic speed of flow system (m.s <sup>-1</sup> )
$We$	Weissenberg number

**Abbreviations:**

2D two-dimensional

3D	three-dimensional
BKC	Blake-Kozeny-Carman
IPM	Invasion Percolation with Memory
MTP	Minimum Threshold Path
TYP	Threshold Yield Pressure
$(\cdot)^T$	matrix transpose
$\overset{\nabla}{\cdot}$	upper convected time derivative

**Note:** units, when relevant, are given in the SI system. Vectors and tensors are marked with boldface. Some symbols may rely on the context for unambiguous identification.

## References

- [1] A.H.P. Skelland. *Non-Newtonian Flow and Heat Transfer*. John Wiley and Sons Inc., 1967. [2](#), [3](#), [10](#), [12](#), [32](#), [70](#)
- [2] R.P. Chhabra; J.F. Richardson. *Non-Newtonian Flow in the Process Industries*. Butterworth Heinemann Publishers, 1999. [2](#), [3](#), [49](#), [61](#)
- [3] R.G. Owens; T.N. Phillips. *Computational Rheology*. Imperial College Press, 2002. [2](#), [7](#), [11](#), [14](#), [16](#), [19](#), [46](#), [50](#), [52](#), [60](#)
- [4] R.G.M. van Os; T.N. Phillips. Spectral element methods for transient viscoelastic flow problems. *Journal of Computational Physics*, 201(1):286–314, 2004. [15](#), [19](#), [70](#)
- [5] A.F. Morais; H. Seybold; H.J. Herrmann; J.S. Andrade Jr. Non-newtonian fluid flow through three-dimensional disordered porous media. *Physical Review Letters*, 103(19):194502, 2009. [2](#)
- [6] R.B. Bird; R.C. Armstrong; O. Hassager. *Dynamics of Polymeric Liquids*, volume 1. John Wiley & Sons, second edition, 1987. [2](#), [7](#), [8](#), [9](#), [12](#), [13](#), [14](#), [15](#), [16](#), [19](#), [37](#), [45](#), [46](#), [49](#), [50](#), [52](#), [55](#), [70](#)
- [7] H.A. Barnes; J.E Hutton; K. Walters. *An introduction to rheology*. Elsevier, 1993. [2](#), [4](#), [7](#), [45](#), [48](#), [49](#), [50](#), [52](#), [55](#), [60](#), [70](#)
- [8] A.A. Collyer. Time dependent fluids. *Physics Education*, 9:38–44, 1974. [3](#), [60](#), [61](#)
- [9] P.J. Carreau; D. De Kee; R.P. Chhabra. *Rheology of Polymeric Systems*. Hanser Publishers, 1997. [8](#), [9](#), [10](#), [12](#), [14](#), [15](#), [19](#), [37](#), [48](#), [49](#), [54](#), [55](#), [60](#), [61](#)
- [10] T.J. Sadowski; R.B. Bird. Non-Newtonian flow through porous media I. Theoretical. *Transactions of the Society of Rheology*, 9(2):243–250, 1965. [23](#), [25](#), [56](#), [58](#)
- [11] J.G. Savins. Non-Newtonian flow through porous media. *Industrial and Engineering Chemistry*, 61(10):18–47, 1969. [54](#), [56](#), [57](#), [58](#)
- [12] T. Sochi; M.J. Blunt. Pore-scale network modeling of Ellis and Herschel-Bulkley fluids. *Journal of Petroleum Science and Engineering*, 60(2):105–124, 2008. [9](#), [10](#), [35](#)

- [13] J.A. Deiber. *Modeling the flow of Newtonian and viscoelastic fluids through porous media*. PhD thesis, Princeton University, 1978. [11](#), [28](#), [46](#), [48](#), [53](#), [58](#)
- [14] M.M. Denn. Issues in viscoelastic fluid mechanics. *Annual Review of Fluid Mechanics*, 22:13–34, 1990.
- [15] M.A. Hulsen. *A discontinuous Galerkin method with splitting applied to viscoelastic flow*. Faculty of Mechanical Engineering and Marine Technology, Delft University of Technology, 1986.
- [16] R. Keunings. Micro-macro methods for the multi-scale simulation of viscoelastic flow using molecular models of kinetic theory. *Rheology Reviews*, pages 67–98, 2004. [11](#), [19](#)
- [17] R.G. Larson. *The Structure and Rheology of Complex Fluids*. Oxford University Press, 1999. [12](#), [16](#), [37](#), [47](#), [48](#), [49](#), [50](#), [52](#), [55](#), [70](#)
- [18] R.G. Larson. *Constitutive Equations for Polymer Melts and Solutions*. Butterworth Publishers, 1988. [12](#), [13](#), [14](#), [15](#), [19](#), [45](#), [46](#), [49](#), [50](#), [70](#)
- [19] J.L. White; A.B. Metzner. Thermodynamic and heat transport considerations for viscoelastic fluids. *Chemical Engineering Science*, 20:1055–1062, 1965. [12](#)
- [20] B. Mena; O. Manero; L.G. Leal. The influence of rheological properties on the slow flow past spheres. *Journal of Non-Newtonian Fluid Mechanics*, 26(2):247–275, 1987. [13](#)
- [21] J.C. Maxwell. On the dynamical theory of gases. *Philosophical Transactions of the Royal Society of London*, 157:49–88, 1867. [13](#)
- [22] H. Jeffreys. *The Earth Its Origin, History and Physical Constitution*. Cambridge University Press, second edition, 1929. [14](#)
- [23] J. Martínez-Mardones; C. Pérez-García. Linear instability in viscoelastic fluid convection. *Journal of Physics: Condensed Matter*, 2(5):1281–1290, 1990. [14](#), [16](#)
- [24] R.I. Tanner. *Engineering Rheology*. Oxford University Press, 2nd edition, 2000. [14](#), [55](#), [70](#)

- [25] M. Sahimi. Nonlinear transport processes in disordered media. *AIChE Journal*, 39(3):369–386, 1993. 15
- [26] A.D. Araújo; W.B. Bastos; J.S. Andrade Jr.; H.J. Herrmann. Distribution of local fluxes in diluted porous media. *Physical Review E*, 74(1):010401, 2006. 15
- [27] N.J. Balmforth; R.V. Craster. *Geophysical Aspects of Non-Newtonian Fluid Mechanics*. Springer, 2001. 16, 37, 60
- [28] D.V. Boger. Viscoelastic flows through contractions. *Annual Review of Fluid Mechanics*, 19:157–182, 1987. 16, 45
- [29] F. Bautista; J.M. de Santos; J.E. Puig; O. Manero. Understanding thixotropic and antithixotropic behavior of viscoelastic micellar solutions and liquid crystalline dispersions. I. The model. *Journal of Non-Newtonian Fluid Mechanics*, 80(2):93–113, 1999. 17, 55
- [30] F. Bautista; J.F.A. Soltero; J.H. Pérez-López; J.E. Puig; O. Manero. On the shear banding flow of elongated micellar solutions. *Journal of Non-Newtonian Fluid Mechanics*, 94(1):57–66, 2000.
- [31] O. Manero; F. Bautista; J.F.A. Soltero; J.E. Puig. Dynamics of worm-like micelles: the Cox-Merz rule. *Journal of Non-Newtonian Fluid Mechanics*, 106(1):1–15, 2002.
- [32] P. Tardy; V.J. Anderson. Current modelling of flow through porous media. *Private communication*, 2005. 17, 30, 33
- [33] J.C. Godfrey. Steady shear measurement of thixotropic fluid properties. *Rheologica Acta*, 12(4):540–545, 1973. 18, 62
- [34] H.A. Barnes. Thixotropy – a review. *Journal of Non-Newtonian Fluid Mechanics*, 70(1):1–33, 1997. 18, 60, 61
- [35] M.A. Hulsen. *Analysis of the equations for viscoelastic flow: Type, boundary conditions, and discontinuities*. Faculty of Mechanical Engineering, Delft University of Technology, 1986. 19
- [36] M.A. Hulsen. *A numerical method for solving steady 2D and axisymmetrical viscoelastic flow problems with an application to inertia effects in contraction*

- flows*. Faculty of Mechanical Engineering, Delft University of Technology, 1990.
- [37] J.S. Andrade Jr.; A.M. Alencar; M.P. Almeida; J. Mendes Filho; S.V. Buldyrev; S. Zapperi; H.E. Stanley; B. Suki. Asymmetric flow in symmetric branched structures. *Physical Review Letters*, 81(4):926–929, 1998.
- [38] J.S. Andrade Jr.; U.M.S. Costa; M.P. Almeida; H.A. Makse; H.E. Stanley. Inertial effects on fluid flow through disordered porous media. *Physical Review Letters*, 82(26):5249–5252, 1999.
- [39] R. Keunings. Finite element methods for integral viscoelastic fluids. *Rheology Reviews*, pages 167–195, 2003. [19](#)
- [40] F. Durst; R. Haas; W. Interthal. The nature of flows through porous media. *Journal of Non-Newtonian Fluid Mechanics*, 22(2):169–189, 1987. [20](#), [57](#), [58](#), [66](#)
- [41] D.L. Johnson; J. Koplik; R. Dashen. Theory of dynamic permeability and tortuosity in fluid-saturated porous media. *Journal of Fluid Mechanics*, 176:379–402, 1987.
- [42] J.S. Andrade; M.P. Almeida; J.M. Filho; S. Havlin; B. Suki; H.E. Stanley. Fluid flow through porous media: The role of stagnant zones. *Physical Review Letters*, 79:3901–3904, 1997. [20](#)
- [43] W.R. Schowalter. *Mechanics of Non-Newtonian Fluids*. Pergamon Press Inc., 1978. [21](#)
- [44] A.V. Shenoy. Darcy-Forchheimer natural, forced and mixed convection heat transfer in non-Newtonian power-law fluid-saturated porous media. *Transport in Porous Media*, 11(3):219–241, 1993. [21](#)
- [45] W. Kozicki; C. Tiu. A unified model for non-Newtonian flow in packed beds and porous media. *Rheologica Acta*, 27(1):31–38, 1988. [22](#), [24](#), [26](#)
- [46] R.P. Chapuis; M. Aubertin. On the use of the Kozeny-Carman equation to predict the hydraulic conductivity of soils. *Canadian Geotechnical Journal*, 40(3):616–628, 2003. [22](#)

- [47] R.P. Chhabra; J. Comiti; I. Machač. Flow of non-Newtonian fluids in fixed and fluidised beds. *Chemical Engineering Science*, 56(1):1–27, 2001. [22](#), [46](#), [48](#), [53](#), [54](#)
- [48] W.M. Jones. The flow of dilute aqueous solutions of macromolecules in various geometries: IV. the Ergun and Jones equations for flow through consolidated beds. *Journal of Physics D: Applied Physics*, 9(5):771–772, 1976. [22](#)
- [49] P. Stevenson. Comment on “Physical insight into the Ergun and Wen & Yu equations for fluid flow in packed and fluidised beds”, by R.K. Niven. *Chemical Engineering Science*, 58(23):5379–5379, 2003. [22](#)
- [50] J.P. Du Plessis. Analytical quantification of coefficients in the Ergun equation for fluid friction in a packed bed. *Transport in Porous Media*, 16(2):189–207, 1994. [22](#)
- [51] J.R.A. Pearson; P.M.J. Tardy. Models for flow of non-Newtonian and complex fluids through porous media. *Journal of Non-Newtonian Fluid Mechanics*, 102(2):447–473, 2002. [23](#), [25](#), [35](#), [47](#), [61](#), [64](#)
- [52] T.J. Sadowski. Non-Newtonian flow through porous media II. Experimental. *Transactions of the Society of Rheology*, 9(2):251–271, 1965. [23](#), [26](#), [58](#), [65](#)
- [53] T.J. Sadowski. *Non-Newtonian flow through porous media*. PhD thesis, University of Wisconsin, 1963. [23](#), [26](#), [54](#), [58](#), [65](#)
- [54] W.B. Gogarty; G.L. Levy; V.G. Fox. Viscoelastic effects in polymer flow through porous media. *SPE 47th Annual Fall Meeting, 8-11 October, San Antonio, Texas, SPE 4025*, 1972. [23](#), [52](#), [53](#), [54](#), [55](#), [58](#), [65](#)
- [55] H.C. Park; M.C. Hawley; R.F. Blanks. The flow of non-Newtonian solutions through packed beds. *SPE 4722*, 1973. [23](#), [37](#), [52](#), [58](#), [65](#)
- [56] H.C. Park. *The flow of non-Newtonian fluids through porous media*. PhD thesis, Michigan State University, 1972. [23](#), [26](#), [65](#)
- [57] H. Pascal. Nonsteady flow through porous media in the presence of a threshold gradient. *Acta Mechanica*, 39(3-4):207–224, 1981. [23](#)
- [58] T.F. Al-Fariss; K.L. Pinder. Flow of a shear-thinning liquid with yield stress through porous media. *SPE 13840*, 1984. [24](#), [37](#), [66](#)

- [59] T.F. Al-Fariss. A new correlation for non-Newtonian flow through porous media. *Computers and Chemical Engineering*, 13(4-5):475–482, 1989. [24](#)
- [60] G.G. Chase; P. Dachavijit. Incompressible cake filtration of a yield stress fluid. *Separation Science and Technology*, 38(4):745–766, 2003. [24](#), [27](#), [67](#)
- [61] W.J. Cannella; C. Huh; R.S. Seright. Prediction of Xanthan rheology in porous media. *SPE Annual Technical Conference and Exhibition, 2-5 October, Houston, Texas, SPE 18089*, 1988. [24](#), [66](#)
- [62] S. Pilitsis; A.N. Beris. Calculations of steady-state viscoelastic flow in an undulating tube. *Journal of Non-Newtonian Fluid Mechanics*, 31(3):231–287, 1989. [25](#), [47](#), [53](#)
- [63] K.S. Sorbie. *Polymer-Improved Oil Recovery*. Blakie and Son Ltd, 1991. [25](#), [26](#), [34](#), [48](#), [57](#), [58](#)
- [64] J.L. Duda; S. Hang; E.E. Klaus. Flow of polymer solutions in porous media: Inadequacy of the capillary model. *Industrial and Engineering Chemistry Fundamentals*, 22(3):299–305, 1983. [26](#)
- [65] A. Zaitoun; N. Kohler. Two-phase flow through porous media: Effect of an adsorbed polymer layer. *SPE Annual Technical Conference and Exhibition, 2-5 October, Houston, Texas, SPE 18085*, 1988. [26](#)
- [66] T.F. Al-Fariss; K.L. Pinder. Flow through porous media of a shear-thinning liquid with yield stress. *Canadian Journal of Chemical Engineering*, 65(3):391–405, 1987. [26](#)
- [67] G.C. Vradis; A.L. Protopapas. Macroscopic conductivities for flow of Bingham plastics in porous media. *Journal of Hydraulic Engineering*, 119(1):95–108, 1993. [27](#), [38](#)
- [68] K.K. Talwar; B. Khomami. Application of higher order finite element methods to viscoelastic flow in porous media. *Journal of Rheology*, 36(7):1377–1416, 1992. [27](#), [52](#), [53](#), [58](#), [59](#)
- [69] A. Souvaliotis; A.N. Beris. Spectral collocation/domain decomposition method for viscoelastic flow simulations in model porous geometries. *Computer Methods in Applied Mechanics and Engineering*, 129(1):9–28, 1996. [27](#)

- [70] C.C. Hua; J.D. Schieber. Viscoelastic flow through fibrous media using the CONNFFESSIT approach. *Journal of Rheology*, 42(3):477–491, 1998. [28](#)
- [71] A. Fadili; P.M.J. Tardy; J.R.A. Pearson. A 3D filtration law for power-law fluids in heterogeneous porous media. *Journal of Non-Newtonian Fluid Mechanics*, 106(2):121–146, 2002. [28](#)
- [72] J.A. Deiber; W.R. Schowalter. Modeling the flow of viscoelastic fluids through porous media. *AIChE Journal*, 27(6):912–920, 1981. [28](#), [47](#), [53](#), [58](#)
- [73] S. Pilitsis; A. Souvaliotis; A.N. Beris. Viscoelastic flow in a periodically constricted tube: The combined effect of inertia, shear thinning, and elasticity. *Journal of Rheology*, 35(4):605–646, 1991. [28](#), [58](#)
- [74] S.H. Momeni-Masuleh; T.N. Phillips. Viscoelastic flow in an undulating tube using spectral methods. *Computers & fluids*, 33(8):1075–1095, 2004. [28](#)
- [75] P.H. Valvatne. *Predictive pore-scale modelling of multiphase flow*. PhD thesis, Imperial College London, 2004. [28](#), [32](#)
- [76] X. Lopez. *Pore-scale modelling of non-Newtonian flow*. PhD thesis, Imperial College London, 2004. [35](#)
- [77] T.M. Sochi. *Pore-Scale Modeling of Non-Newtonian Flow in Porous Media*. PhD thesis, Imperial College London, 2007. [28](#), [30](#), [32](#), [33](#), [35](#), [39](#), [41](#), [64](#)
- [78] M.J. Blunt. Flow in porous media - pore-network models and multiphase flow. *Colloid and Interface Science*, 6(3):197–207, 2001. [29](#)
- [79] M.J. Blunt; M.D. Jackson; M. Piri; P.H. Valvatne. Detailed physics, predictive capabilities and macroscopic consequences for pore-network models of multiphase flow. *Advances in Water Resources*, 25(8-12):1069–1089, 2002. [29](#)
- [80] Taha Sochi. Computational techniques for modeling non-Newtonian flow in porous media. *International Journal of Modeling, Simulation, and Scientific Computing*, 1(2):239–256, 2010. [29](#)
- [81] M. Sahimi; D. Stauffer. Efficient simulation of flow and transport in porous media. *Chemical Engineering Science*, 46(9):2225–2233, 1991.

- [82] D.H. Rothman. Lattice-gas models of phase separation: interfaces, phase transitions, and multiphase flow. *Reviews of Modern Physics*, 66(4):1417–1479, 1994.
- [83] B. Ferréol; D.H. Rothman. Lattice-Boltzmann simulations of flow through Fontainebleau sandstone. *Transport in Porous Media*, 20(1-2):3–20, 1995. [29](#)
- [84] P.E. Øren; S. Bakke; O.J. Amtzen. Extending predictive capabilities to network models. *SPE Annual Technical Conference and Exhibition, San Antonio, Texas*, (SPE 38880), 1997. [32](#)
- [85] P.E. Øren; S. Bakke. Reconstruction of Berea sandstone and pore-scale modelling of wettability effects. *Journal of Petroleum Science and Engineering*, 39(3-4):177–199, 2003. [32](#)
- [86] J.W. Ruge; K. Stüben. *Multigrid Methods: Chapter 4 (Algebraic Multigrid)*, *Frontiers in Applied Mathematics*. SIAM, 1987. [33](#)
- [87] K.S. Sorbie; P.J. Clifford; E.R.W. Jones. The rheology of pseudoplastic fluids in porous media using network modeling. *Journal of Colloid and Interface Science*, 130(2):508–534, 1989. [34](#)
- [88] D.A. Coombe; V. Oballa; W.L. Buchanan. Scaling up the non-Newtonian flow characteristics of polymers, foams, and emulsions. *12th SPE Symposium on Reservoir Simulation, 28 February - 3 March, New Orleans, LA, SPE 25237*, 1993. [34](#)
- [89] C. Shah; H. Kharabaf; Y.C. Yortsos. Immiscible displacements involving power-law fluids in porous media. *Proceedings of the Seventh UNITAR International Conference on Heavy Crude and Tar Sands, Beijing, China*, 1998. [34](#)
- [90] J.P. Tian; K.L. Yao. Immiscible displacements of two-phase non-Newtonian fluids in porous media. *Physics Letters A*, 261(3-4):174–178, 1999. [35](#)
- [91] C.D. Tsakiroglou. A methodology for the derivation of non-Darcian models for the flow of generalized Newtonian fluids in porous media. *Journal of Non-Newtonian Fluid Mechanics*, 105(2-3):79–110, 2002. [35](#)
- [92] C.D. Tsakiroglou. Correlation of the two-phase flow coefficients of porous media with the rheology of shear-thinning fluids. *Journal of Non-Newtonian Fluid Mechanics*, 117(1):1–23, 2004. [35](#)

- [93] C.D. Tsakiroglou; M. Theodoropoulou; V. Karoutsos; D. Papanicolaou; V. Sygouni. Experimental study of the immiscible displacement of shear-thinning fluids in pore networks. *Journal of Colloid and Interface Science*, 267(1):217–232, 2003. [35](#)
- [94] X. Lopez; P.H. Valvatne; M.J. Blunt. Predictive network modeling of single-phase non-Newtonian flow in porous media. *Journal of Colloid and Interface Science*, 264(1):256–265, 2003. [35](#)
- [95] X. Lopez; M.J. Blunt. Predicting the impact of non-Newtonian rheology on relative permeability using pore-scale modeling. *SPE Annual Technical Conference and Exhibition, 26-29 September, Houston, Texas, SPE 89981*, 2004. [35](#)
- [96] M.T. Balhoff; K.E. Thompson. Modeling the steady flow of yield-stress fluids in packed beds. *AIChE Journal*, 50(12):3034–3048, 2004. [35](#)
- [97] M.T. Balhoff; K.E. Thompson. A macroscopic model for shear-thinning flow in packed beds based on network modeling. *Chemical Engineering Science*, 61(2):698–719, 2006. [67](#)
- [98] M.T. Balhoff. *Modeling the flow of non-Newtonian fluids in packed beds at the pore scale*. PhD thesis, Louisiana State University, 2005. [35](#), [39](#), [67](#)
- [99] C.L. Perrin; P.M.J. Tardy; S. Sorbie; J.C. Crawshaw. Experimental and modeling study of Newtonian and non-Newtonian fluid flow in pore network micromodels. *Journal of Colloid and Interface Science*, 295(2):542–550, 2006. [35](#), [67](#)
- [100] W.R. Rossen; C.K. Mamun. Minimal path for transport in networks. *Physical Review B*, 47(18):11815–11825, 1993. [36](#), [44](#)
- [101] M. Chen; Y.C. Yortsos; W.R. Rossen. A pore-network study of the mechanisms of foam generation. *SPE Annual Technical Conference and Exhibition, 26-29 September, Houston, Texas, SPE 90939*, 2004. [36](#)
- [102] M. Chen; Y.C. Yortsos; W.R. Rossen. Insights on foam generation in porous media from pore-network studies. *Colloids and Surfaces A: Physicochemical and Engineering Aspects*, 256(2-3):181–189, 2005. [41](#)

- [103] M. Chen; W.R. Rossen; Y.C. Yortsos. The flow and displacement in porous media of fluids with yield stress. *Chemical Engineering Science*, 60(15):4183–4202, 2005. [36](#), [40](#), [41](#), [44](#)
- [104] H.A. Barnes. The yield stress—a review or ‘ $\pi\alpha\nu\tau\alpha\rho\varepsilon\iota$ ’—everything flows? *Journal of Non-Newtonian Fluid Mechanics*, 81(1):133–178, 1999. [37](#)
- [105] T. Sochi. Modelling the flow of yield-stress fluids in porous media. *Transport in Porous Media*, DOI: 10.1007/s11242-010-9574-z, 2010. [37](#), [39](#)
- [106] J. Bear. *Dynamics of Fluids in Porous Media*. American Elsevier, 1972. [38](#)
- [107] S. Liu; J.H. Masliyah. On non-Newtonian fluid flow in ducts and porous media - Optical rheometry in opposed jets and flow through porous media. *Chemical Engineering Science*, 53(6):1175–1201, 1998. [38](#)
- [108] A. Vikhansky. Lattice-Boltzmann method for yield-stress liquids. *Journal of Non-Newtonian Fluid Mechanics*, doi:10.1016/j.jnnfm.2007.09.001, 2007. [39](#)
- [109] A.P. Sheppard M.A. Knackstedt, M. Sahimi. Invasion percolation with long-range correlations: first-order phase transition and nonuniversal scaling properties. *Physical Review E*, 61(5):4920–4934, 2000. [40](#)
- [110] S. Roux; A. Hansen. A new algorithm to extract the backbone in a random resistor network. *Journal of Physics A*, 20:L1281–L1285, 1987. [40](#)
- [111] H. Kharabaf; Y.C. Yortsos. Invasion percolation with memory. *Physical Review*, 55(6):7177–7191, 1997. [40](#), [41](#)
- [112] R. Chandler; J. Koplik; K. Lerman; J.F. Willemsen. Capillary displacement and percolation in porous media. *Journal of Fluid Mechanics*, 119:249–267, 1982. [41](#)
- [113] A. Klemm; H.-P. Müller; R. Kimmich. Evaluation of fractal parameters of percolation model objects and natural porous media by means of nmr microscopy. *Physica A*, 266(1-4):242–246, 1999.
- [114] J.S. Andrade; S.V. Buldyrev; N.V. Dokholyan; S. Havlin; P.R. King; Y. Lee; G. Paul; E. Stanley. Flow between two sites on a percolation cluster. *Physical Review E*, 62:8270–8281, 2000.

- [115] H.A. Makse; J.S. Andrade Jr; H.E. Stanley. Tracer dispersion in a percolation network with spatial correlations. *Physical Review E*, 61(1):583–586, 2000.
- [116] A. Klemm; R. Kimmich; M. Weber. Flow through percolation clusters: Nmr velocity mapping and numerical simulation study. *Physical Review E*, 63(4):041514, 2001. [41](#)
- [117] V.I. Selyakov; V.V. Kadet. *Percolation Models for Transport in Porous Media with Applications to Reservoir Engineering*. Kluwer Academic Publishers, 1996. [43](#)
- [118] M. Sahimi. *Applications of Percolation Theory*. Taylor and Francis, 1994.
- [119] J. S. Andrade Jr.; D.A. Street; T. Shinohara; Y. Shibusa; Y. Arai. Percolation disorder in viscous and nonviscous flow through porous media. *Physical Review E*, 51(6):5725–5731, 1995.
- [120] M. Sahimi; S. Mukhopadhyay. Scaling properties of a percolation model with long-range correlations. *Physical Review E*, 54(4):3870–3880, 1996.
- [121] A.D. Araújo; T.F. Vasconcelos; A.A. Moreira; L.S. Lucena; J.S. Andrade Jr. Invasion percolation between two sites. *Physical Review E*, 72(4):041404, 2005. [43](#)
- [122] W.R. Rossen; P.A. Gauglitz. Percolation theory of creation and mobilization of foam in porous media. *A.I.Ch.E. Journal*, 36(8):1176–1188, 1990. [44](#)
- [123] W.M. Jones; S.P. Ho. The flow of dilute aqueous solutions of macromolecules in various geometries: VII. Mechanisms of resistance in porous media. *Journal of Physics D: Applied Physics*, 12(3):383–393, 1979. [46](#)
- [124] E.H. Wissler. Viscoelastic effects in the flow of non-Newtonian fluids through a porous medium. *Industrial & Engineering Chemistry Fundamentals*, 10(3):411–417, 1971. [46](#), [54](#), [58](#)
- [125] R.J. Marshall; A.B. Metzner. Flow of viscoelastic fluids through porous media. *Industrial & Engineering Chemistry Fundamentals*, 6(3):393–400, 1967. [47](#), [53](#), [55](#), [56](#), [65](#)
- [126] D.L. Dauben; D.E. Menzie. Flow of polymer solutions through porous media. *Journal of Petroleum Technology, SPE 1688-PA*, pages 1065–1073, 1967. [54](#), [57](#)

- [127] P.R.S. Mendes; M.F. Naccache. A constitutive equation for extensional-thickening fluids flowing through porous media. *Proceedings of 2002 ASME International Mechanical Engineering Congress & Exposition, November 17-22, New Orleans, Louisiana, USA, 2002.* 49, 57, 59
- [128] J.P. Plog; W.M. Kulicke. Flow behaviour of dilute hydrocolloid solutions through porous media. Influence of molecular weight, concentration and solvent. *Institute of Technical and Macromolecular Chemistry, University of Hamburg, 2002.* 47
- [129] T. Sochi. Pore-scale modeling of viscoelastic flow in porous media using a Bautista-Manero fluid. *International Journal of Heat and Fluid Flow, 30(6):1202–1217, 2009.* 47, 64
- [130] N. Phan-Thien; M.M.K. Khan. Flow of an Oldroyd-type fluid through a sinusoidally corrugated tube. *Journal of Non-Newtonian Fluid Mechanics, 24(2):203–220, 1987.* 47
- [131] M. Sahimi. Flow phenomena in rocks: from continuum models to fractals, percolation, cellular automata, and simulated annealing. *Reviews of Modern Physics, 65(4):1393–1534, 1993.*
- [132] J.S. Andrade Jr.; A.D. Araújo; H.E. Stanley; U.M.S. Costa. Fluid flow through disordered porous media. *Fractals-Complex Geometry Patterns and Scaling in Nature and Society, 11:301–312, 2003.* 47
- [133] D.C.H. Cheng; N.I. Heywood. Flow in pipes. I. Flow of homogeneous fluids. *Physics in Technology, 15(5):244–251, 1984.* 48, 50
- [134] A.S. Lodge. *Elastic Liquids An Introductory Vector Treatment of Finite-strain Polymer Rheology.* Academic Press, 1964. 49
- [135] M.J. Crochet; K. Walters. Numerical methods in non-Newtonian fluid mechanics. *Annual Review of Fluid Mechanics, 15(241-260), 1983.* 50
- [136] A. Souvaliotis; A.N. Beris. Applications of domain decomposition spectral collocation methods in viscoelastic flows through model porous media. *Journal of Rheology, 36(7):1417–1453, 1992.* 53
- [137] A.K. Podolsak; C. Tiu; T.N. Fang. Flow of non-Newtonian fluids through tubes with abrupt expansions and contractions (square wave tubes). *Journal of Non-Newtonian Fluid Mechanics, 71(1):25–39, 1997.* 53

- [138] F.A.L. Dullien. Single phase flow through porous media and pore structure. *The Chemical Engineering Journal*, 10(1):1–34, 1975. [54](#)
- [139] G.J. Hirasaki; G.A. Pope. Analysis of factors influencing mobility and adsorption in the flow of polymer solution through porous media. *SPE 47th Annual Fall Meeting, 8-11 October, San Antonio, Texas, SPE 4026*, 1972. [55](#), [58](#)
- [140] M.F. Letelier; D.A. Siginer; C. Caceres. Pulsating flow of viscoelastic fluids in straight tubes of arbitrary cross-section-Part I: longitudinal field. *International Journal of Non-Linear Mechanics*, 37(2):369–393, 2002. [56](#)
- [141] C. Chmielewski; C.A. Petty; K. Jayaraman. Crossflow of elastic liquids through arrays of cylinders. *Journal of Non-Newtonian Fluid Mechanics*, 35(2-3):309–325, 1990. [58](#), [66](#)
- [142] C. Chmielewski; K. Jayaraman. The effect of polymer extensibility on cross-flow of polymer solutions through cylinder arrays. *Journal of Rheology*, 36(6):1105–1126, 1992.
- [143] C. Chmielewski; K. Jayaraman. Elastic instability in crossflow of polymer solutions through periodic arrays of cylinders. *Journal of Non-Newtonian Fluid Mechanics*, 48(3):285–301, 1993. [58](#), [66](#)
- [144] A.A. Garrouch. A viscoelastic model for polymer flow in reservoir rocks. *SPE Asia Pacific Oil and Gas Conference and Exhibition, 20-22 April, Jakarta, Indonesia, SPE 54379*, 1999. [59](#)
- [145] T. Koshiha; N. Mori; K. Nakamura; S. Sugiyama. Measurement of pressure loss and observation of the flow field in viscoelastic flow through an undulating channel. *Journal of Rheology*, 44(1):65–78, 2000. [59](#)
- [146] B. Khuzhayorov; J.-L. Auriault; P. Royer. Derivation of macroscopic filtration law for transient linear viscoelastic fluid flow in porous media. *International Journal of Engineering Science*, 38(5):487–504, 2000. [59](#)
- [147] X. Huifen; Y. XiangAn; W. Dexi; L. Qun; Z. Xuebin. Prediction of IPR curve of oil wells in visco-elastic polymer solution flooding reservoirs. *SPE Asia Pacific Improved Oil Recovery Conference, 6-9 October, Kuala Lumpur, Malaysia, SPE 72122*, 2001. [59](#)

- [148] V. Dolejš; J. Cakl; B. Šiška; P. Doleček. Creeping flow of viscoelastic fluid through fixed beds of particles. *Chemical Engineering and Processing*, 41(2):173–178, 2002. [59](#)
- [149] M.P. Escudier; F. Presti. Pipe flow of a thixotropic liquid. *Journal of Non-Newtonian Fluid Mechanics*, 62(2):291–306, 1996. [60](#), [61](#), [62](#)
- [150] K. Dullaert; J. Mewis. Thixotropy: Build-up and breakdown curves during flow. *Journal of Rheology*, 49(6):1213–1230, 2005. [60](#), [61](#), [62](#)
- [151] D.C. Cheng; F. Evans. Phenomenological characterization of the rheological behaviour of inelastic reversible thixotropic and antithixotropic fluids. *British Journal of Applied Physics*, 16(11):1599–1617, 1965. [60](#), [61](#), [64](#)
- [152] J. Mewis. Thixotropy - a general review. *Journal of Non-Newtonian Fluid Mechanics*, 6(1):1–20, 1979. [60](#), [61](#), [62](#)
- [153] D.D. Joye; G.W. Poehlein. Characteristics of thixotropic behavior. *Journal of Rheology*, 15(1):51–61, 1971. [61](#), [62](#)
- [154] J. Billingham; J.W.J. Ferguson. Laminar, unidirectional flow of a thixotropic fluid in a circular pipe. *Journal of Non-Newtonian Fluid Mechanics*, 47:21–55, 1993.
- [155] D. Pritchard; J.R.A. Pearson. Viscous fingering of a thixotropic fluid in a porous medium or a narrow fracture. *Journal of Non-Newtonian Fluid Mechanics*, 135(2-3):117–127, 2006. [61](#), [64](#)
- [156] S. Wang; Y. Huang; F. Civan. Experimental and theoretical investigation of the Zaoyuan field heavy oil flow through porous media. *Journal of Petroleum Science and Engineering*, 50(2):83–101, 2006. [64](#), [68](#)
- [157] D.A. White. Non-Newtonian flow in stratified porous media and in axisymmetric geometries. *Chemical Engineering Science*, 23(3):243–251, 1968. [65](#)
- [158] D. Teeuw; F.T. Hesselink. Power-law flow and hydrodynamic behaviour of biopolymer solutions in porous media. *SPE Fifth International Symposium on Oilfield and Geothermal Chemistry, May 28-30, Stanford, California, SPE 8982*, 1980. [65](#)

- [159] P. Vogel; G.A. Pusch. Some aspects of the injectivity of non-Newtonian fluids in porous media. *European Symposium on EOR, 21-22 September, Bournemouth, UK, 1981.* 66
- [160] K.S. Sorbie; A. Parker; P.J. Clifford. Experimental and theoretical study of polymer flow in porous media. *SPE Reservoir Engineering, SPE 14231, 2(3):281-304, 1987.* 66
- [161] R.P. Chhabra; B.K. Srinivas. Non-Newtonian (purely viscous) fluid flow through packed beds: effect of particle shape. *Powder Technology, 67:15-19, 1991.* 66
- [162] A.J.P. Fletcher; S.R.G. Flew; S.P. Lamb; T. Lund; E. Bjørnstad; A. Stavland; N.B. Gjøvikli. Measurements of polysaccharide polymer properties in porous media. *SPE International Symposium on Oilfield Chemistry, 20-22 February, Anaheim, California, SPE 21018, 1991.* 66
- [163] S. Hejri; G.P. Willhite; D.W. Green. Development of correlations to predict biopolymer mobility in porous media. *SPE Reservoir Engineering, SPE 17396, 6(1):91-98, 1991.* 67
- [164] N. Sabiri; J. Comiti. Pressure drop in non-Newtonian purely viscous fluid flow through porous media. *Chemical Engineering Science, 50(7):1193-1201, 1995.* 67
- [165] R.A. Saunders; C. Lekakou; M.G. Bader. Compression in the processing of polymer composites 2. Modelling of the viscoelastic compression of resin-impregnated fibre networks. *Composites Science and Technology, 59(10):1483-1494, 1999.* 67
- [166] P. Kuzhir; G. Bossis; V. Bashtovoi; O. Volkova. Flow of magnetorheological fluid through porous media. *European Journal of Mechanics - B/Fluids, 22(4):331-343, 2003.* 67
- [167] M.V. D'Angelo; E. Fontana; R. Chertcoff; M. Rosen. Retention phenomena in non-Newtonian fluids flow. *Physica A, 327(1-2):44-48, 2003.* 67
- [168] U.M. Scheven; J.P. Crawshaw; V.J. Anderson; R. Harris; M.L. Johns; L.F. Gladden. A cumulant analysis for non-Gaussian displacement distributions in Newtonian and non-Newtonian flows through porous media. *Magnetic Resonance Imaging, 25(4):513-516, 2007.* 68

- [169] D.V. Boger. A highly elastic constant-viscosity fluid. *Journal of Non-Newtonian Fluid Mechanics*, 3(1):87–91, 1977. [70](#)
- [170] F.M. White. *Viscous Fluid Flow*. McGraw Hill Inc., second edition, 1991. [70](#)

## Index

- Adsorption, 32, 54
- Ballotini, 68
- Bautista-Manero, 16, 17, 35, 64
- Bentheim, 66
- Berea, 32, 66
- Bingham, 11, 27, 35, 37, 39, 67
- Blake, 21, 22, 24, 26, 77
- Boger, 14, 16, 73, 74
- Carbopol, 65, 67
- Carbowax, 65
- Carboximethylcellulose, 67
- Carboxymethylcellulose, 23, 58, 65, 66
- Carman, 21, 22, 26, 77
- Carreau, 7, 9, 10, 34, 35, 66, 67
- Casson, 37
- Clashach, 67
- Converging-Diverging, 3, 4, 6, 24, 25, 27–30, 33, 34, 39, 47, 48, 52, 53, 58, 59, 69
- Darcy, 20–24, 26, 28, 33, 58, 59, 65, 76
- Deborah number, 45, 58, 65, 73, 76
- Dilatancy, 3, 53, 54, 57
- Dilatant, 7, 11, 54, 57, 58
- Diverging-Converging, 57
- Ellis, 7–9, 19, 23, 26, 35, 65, 67, 75
- Elvanol, 65
- Ergun, 21–24, 66
- Extension-thickening, 11, 47, 48, 57, 59
- Flocon, 66, 67
- Fredrickson, 16, 17, 75, 76
- Friction factor, 22, 23, 66
- Giesekus, 16
- Godfrey, 18, 75
- Guar, 67
- Herschel-Bulkley, 7, 10, 11, 23, 24, 26, 35, 37, 65, 66, 68, 76
- Hook, 14, 45
- Hookean, 46, 73
- Hydroxyethylcellulose, 65, 66
- Invasion Percolation with Memory, 41, 77
- Jeffreys, 14–16
- Kozeny, 21, 22, 24, 26, 58, 77
- Maxwell, 13–15, 45
- Mechanical trapping, 32
- Meter, 35
- Mooney, 59
- Natrosol, 65
- Navier-Stokes, 19, 21, 22
- Newton, 11, 14, 45
- Newtonian, 1, 2, 4, 7, 9–11, 14, 16, 17, 19, 21, 23, 26, 29, 30, 32, 35, 38, 45–47, 49, 50, 52, 53, 57, 59, 63, 67, 68, 73
- Non-Newtonian, 1–4, 7, 10, 19–23, 26–30, 32, 34, 35, 37, 38, 45, 47, 49, 53, 54, 58, 61, 65–69, 73
- Oldroyd, 12, 13, 15, 59
- Oldroyd-B, 13, 15, 16, 19, 27, 28, 59
- Ostwald-de Waele, 8
- Percolation, 40, 41, 43, 44

Phan-Thien-Tanner, 16  
 Poiseuille, 24, 32, 33  
 Polyacrylamide, 35, 65–67  
 Polyisobutylene, 58, 65, 66  
 Polymethylcellulose, 65  
 Polysaccharide, 66  
 Power-law, 7–9, 11, 28, 35, 59, 65–67, 76  
 Pseudoplastic, 7, 11  
  
 Rabinowitsch, 59  
 Raschig, 66  
 Retention, 32, 39, 54, 56, 57, 67  
 Reynolds number, 21, 22, 27, 32, 58, 73, 76  
 Rheopectic, 17, 18, 60  
 Rheopexy, 4, 17, 18, 60, 61  
  
 Sand pack, 32, 66–68  
 Scleroglucan, 66, 67  
 Shear-thickening, 3, 4, 7, 8, 11, 35, 50, 57, 60  
 Shear-thinning, 3, 4, 7–9, 11, 17, 28, 34, 35, 45, 48, 50, 56–58, 60, 66, 68  
 Steady-state, 3, 15, 19, 27, 28, 30, 31, 33, 46, 53–56, 60  
 Stretch-thickening, 57, 59  
 Stretched Exponential Model, 18, 75, 76  
 Superficial velocity, 21, 22  
  
 Tension-thickening, 50, 52  
 Tension-thinning, 50, 52  
 Thixotropic, 4, 17, 18, 31, 35, 60–64, 68  
 Thixotropy, 4, 16, 17, 35, 60–62  
 Time-dependent, 1–4, 7, 11, 17, 18, 23, 27, 31, 45, 55, 56, 60, 61, 63, 64  
 Time-independent, 1–5, 7, 8, 10, 32, 35, 60  
 Transient, 17, 19, 23, 27, 54, 55, 59, 62  
 Trouton, 47, 48, 50, 76  
 UCM, 16  
 Upper Convected Maxwell, 13, 14, 27, 59  
 Viscoelastic, 3–6, 11–15, 17, 23–25, 27, 28, 33, 35, 45–47, 49, 50, 52–59, 61, 62, 64, 65, 67, 68, 70–73  
 Viscoelasticity, 4, 11–13, 16, 31, 35, 39, 45, 46, 54, 60, 61, 64, 70–72  
 Viscoplastic, 37  
 Wall exclusion, 32  
 Weissenberg number, 45, 73, 76  
 Xanthan, 66, 68  
 Yield-stress, 1–3, 7–11, 23–25, 27, 31, 33–44, 68, 76